2016

A comparison of slip measurement techniques

Raja Bharath Vangapattu

ABSTRACT

A COMPARISON OF SLIP MEASUREMENT TECHNIQUES.

Raja Bharath Vangapattu, M.S.
Department of Electrical Engineering
Northern Illinois University, 2016
Dr. Donald S. Zinger, Director

This thesis mainly deals with the slip frequency measurement of an induction motor using two slip measurement techniques and comparison of the techniques used. Direct torque control scheme was used to control the speed and torque of the machine. The slip is calculated using direct torque control equation and also through the rotor flux derivatives. The circuit was built and simulated in Matlab R2015A.

NORTHERN ILLINOIS UNIVERSITY

DEKALB, ILLINOIS

DECEMBER 2016

A COMPARISON OF SLIP MEASUREMENT TECHNIQUES

BY

RAJA BHARATH VANGAPATTU

A THESIS SUBMITTED TO THE GRADUATE SCHOOL IN

PARTIAL FULFILLMENT OF THE REQUIREMENTS

FOR THE DEGREE

MASTER OF SCIENCE

DEPARTMENT OF ELECTRICAL ENGINEERING

Thesis Director:

Donald S. Zinger

ACKNOWLEDGEMENTS

At this moment, I take this opportunity to express my gratitude to the people who have been influential in the successful completion of this thesis.

I would sincerely thank my mentor and guide, Dr. Donald S. Zinger, for his continuous support throughout my master's program, without whom this thesis wouldn't have been possible. I owe a great debt to him.

I would like to thank Dr. Michael Haji Sheik and Dr. Veysel Demir for serving on my committee.

I would also like to express my gratitude towards Ms. Sindhuja Devabakthuni for her encouragement and support in difficult times and patting my back. Also for bearing me these years.

DEDICATION

To Mum, Dad, Sissy, Piggy and friends with love and affection.

TABLE OF CONTENTS

LIST OF FIGURES

Figure

CHAPTER 1

INTRODUCTION AND BACKGROUND

Motivation

Because of their reliability, low cost and robust structure, induction machines are the most widely used electrical machines in industrial applications, but they have some serious problems with the speed control and efficiency. As an effort to improve, the improvised direct torque control scheme is implemented to control the torque and speed of the machine.

Slip, which is responsible for torque generation in induction machines, has also some serious disadvantages. The slip is high at low loads and low speed. When the slip is high, the slip draws more current in the rotor, hence giving high starting torques. These high starting torques may be a problem in load sharing when two or more motors are connected. Also, the slip should be maintained low to achieve maximum efficiency of the machine.

Various methods like slip compensation have been used to control the slip in the machines. The slip must be measured accurately to implement these slip-controlling techniques. Hence, two techniques were discussed in this thesis. A comparison of both the techniques is also included.

Thesis Organization

Chapter 2 contains a good general overview of the induction motor, slip and its effects on the performance of the machine.

Chapter 3 deals with the DTC technique used to control the torque and speed of the motor.

Chapter 4 contains the proposed model for the slip speed measurement

Chapter 5 talks about the two different slip frequency measuring techniques and comparing both the techniques.

Chapter 6 contains results, conclusions and future enhancements that can be applied to proposed design.

CHAPTER 2

INDUCTION MOTOR

An induction machine is typically run as a motor as it lacks the desired characters of a generator. It runs on the principle of Faraday's law of electromagnetic induction.

It has a ferromagnetic cylindrical structure comprising a stationary stator and a wound or slotted rotor which is the rotating component. In a three-phase induction motor, the stator has three separate windings where each phase is supplied with voltages to produce rotating magnetic field (RMF). The relative speed between the stator's RMF and the rotor will result in an induced current in the rotor conductors.

The induced current in the current in the rotor will produce an alternating flux around it. According to Lenz's law, the direction of the induced current will tend to oppose the cause of its production and hence the rotor tries to match the RMF of the stator. However, the rotor never achieves the synchronous speed of the machine.

Synchronous Speed or Electrical Speed:

The no load rotational speed of the stator is the synchronous speed of the machine in rpm.

$$Ns = \frac{120*f}{p} \tag{2.1}$$

here, f = frequency of supply

P = number of stator poles.

Slip:

If the rotor matches the synchronous speed, there will not be any relative speed between the stator flux and the rotor, resulting in no induced rotor current and no torque. This is a reason why the rotor rotates at speed is always less the synchronous speed (Manney, 2013). Slip is the difference between the electrical speed of stator (N_s) and the actual speed of the rotor (N_r). Slip has a key role in an induction motor. The efficiency of an induction motor is estimated with the slip percentage which is given as

$$S\% = \frac{Ns - Nr}{Ns} * 100 \tag{2.2}$$

Slip which is essential for torque production increases with increasing load (Manney, 2013).

The induced EMF in the machine can be represented as proportional to slip speed, which is nothing but the difference between synchronous speed and the speed of the rotor. This can be expressed as

$$e_2 \propto Ns - Nr \tag{2.3}$$

The rotor current induced is directly proportional to the induced EMF, thus giving us the relation

$$i_2 \propto e_2 \tag{2.4}$$

The torque developed in the motor is directly proportional to the induced rotor current

$$T \propto i_2 \tag{2.5}$$

Therefore, $$T \propto (\text{Ns} - \text{Nr}) \quad \text{or} \quad \text{T} = \text{K*Ns}\left(\frac{Ns-Nr}{Ns}\right) \quad \text{or} \quad \text{T} = \text{K}_1\text{*S} \tag{2.6}$$

here K_1 is constant.

Hence, from the above equations deduced, torque is proportional to slip

$$\text{T} \propto \text{S} \tag{2.7}$$

Thus, for a high value of the slip, the induced EMF and the rotor current will be high. As a result, the electromagnetic torque developed will be high (Slip Speed in an Induction Motor, n.d.).

At no-load conditions, the induction motor requires small torque to overcome mechanical and iron losses, so slip is small. At loaded condition, high torque is required to drive the load. As the speed of the rotor decreases, the slip speed increases. The main contribution of slip is that it adjusts itself to such a value to produce the required driving torque under normal operation (Slip Speed in an Induction Motor, n.d.).

But, since high slip draws high currents, the machine may overheat. And hence, the optimum slip should be maintained for the efficient running of the machine.

CHAPTER 3

INDUCTION MOTOR DIRECT TORQUE CONTROL

Field-Oriented Control Scheme:

Field-oriented controllers (FOC) are among the widely used controllers in the industrial applications. FOCs work on the transformation of the motor model variables to the reference frame, which rotates according to a chosen vector aligned with the flux of the rotor (Nemec, Nedeljkovic, & Ambrozic, 2007).

FOC operates in a rotating dq reference frame that is synchronized to the rotor flux. The torque and flux are decoupled in a way that the rotor flux magnitude is controlled by the d-axis component of the stator current and the q-axis component controls the output torque (Karlis, Kiriakopoulos, & Papadopoulos, 2006). A proportional-integral (PI) controller is needed to regulate the torque and flux control loops superimposed upon the current control loops (Nemec, Nedeljkovic, & Ambrozic, 2007).

FOCs are classified into two: direct FOC scheme and indirect FOC scheme.

In DFOC scheme, the vector of the rotor flux is either measured by a flux sensor placed in the air-gap or by the voltage equations. In IFOC, the vector of rotor flux is determined using the FOC equations which require rotor speed. Between both, IFOC is more chosen as it can easily operate through the speed range typically from zero to high speed in closed loop (SARUTECH, 2016). A basic block diagram of IFOC is shown in Fig 3.1.

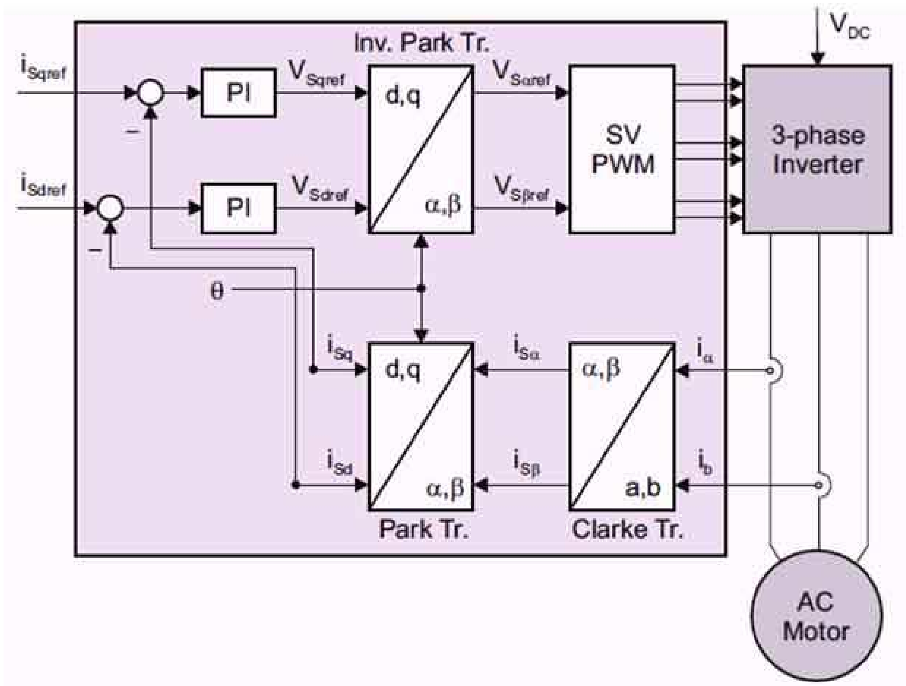

Fig: 3.1 Basic IFOC block diagram (SARUTECH, 2016).

Direct Torque Control Scheme:

FOC has a serious drawback in that it depends on the motor parameters. The time constant of the rotor is difficult to measure precisely and varies with temperature. Direct torque control is one robust technique that is able to produce very fast torque and flux control with respect to motor parameters. Even if the DTC is simple, it all has a good torque control in steady-state and transient conditions (Chikhi , Mohamed , & Chikh, 2010).

The following relations are used (Mathworks, n.d.):

$$\varphi_{ds} = \int (V_{ds} - R_s i_{ds})\, dt \tag{3.1}$$

$$\varphi_{qs} = \int \int (V_{qs} - R_s i_{qs})\, dt \tag{3.2}$$

$$\varphi_{s^\wedge} = \sqrt{(\varphi ds)^\wedge 2 + (\varphi qs)^\wedge 2} \angle \operatorname{atan} \frac{\varphi qs}{\varphi ds} \tag{3.3}$$

$$T_e = 1.5 * p\,(\varphi_{ds} i_{qs} - \varphi_{qs} i_{ds}) \tag{3.4}$$

<u>Direct Torque Controller Block:</u>

As the circuit is built and simulated in Matlab R2015A, let's see what the DTC block looks like in the software. Fig. 3.2 shows the DTC block used from Matlab.

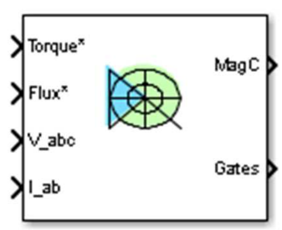

Fig. 3.2 DTC block in Matlab.

Now discussing about the input and output ports of the DTC block, it has four input and two output ports; the torque, flux, V_abc and I_ab serves as input ports and MagC and Gates port serve as output ports.

The torque and flux references to the DTC block are essentially provided by the speed controller. V_abc is the three-phase voltages of the induction motor. I_ab represents line currents Ia and Ib.

MagC which is connected to the MagC of the speed controller is a binary signal indicator which decides if the machine is magnetized enough to start or not (MathWorks, n.d.).

Gate pulses as an output are then given to drive the three-phase inverter.

There are six separate blocks in the DTC block where the data is processed and the output is essentially gate pulses fed to the inverter.

Fig. 3.3 shows the basic DTC scheme.

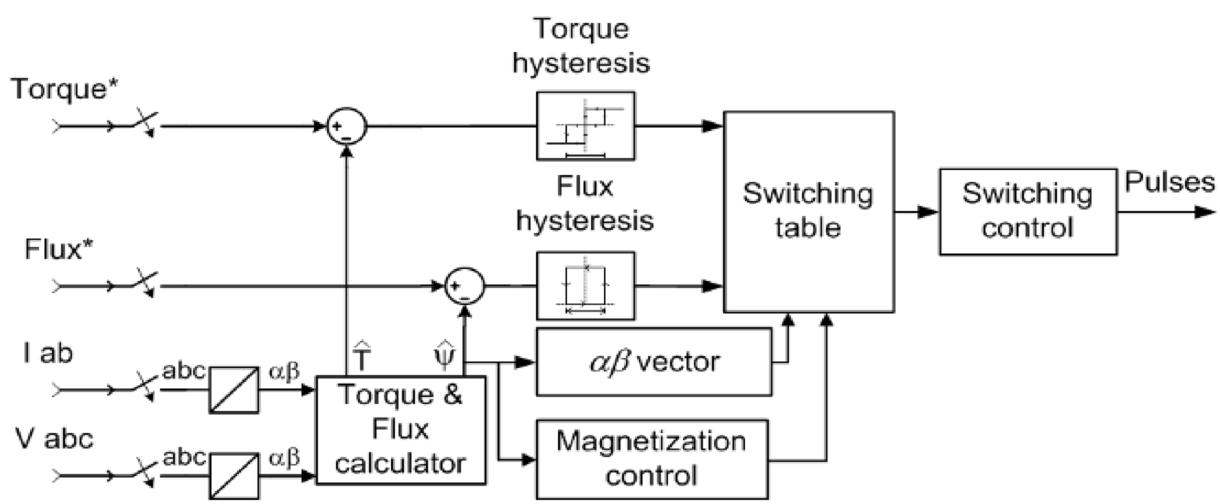

Fig. 3.3 DTC scheme. (Mathworks, n.d.)

As observed from Fig. 3.3, DTC has mainly six blocks, consisting of the following:

1. Torque and flux calculator block that estimates the motor flux αβ components and the electromagnetic torque. (MathWorks, n.d.)

2. The αβ vector block which finds the sector of the αβ plane where the vector of the flux lies. (MathWorks, n.d.)

3. The flux and torque hysteresis block contains hysteresis comparator for flux torque control. (MathWorks, n.d.)

4. The switching table block selects a vector for specific voltage in accordance with the output of the flux and torque hysteresis comparators. This block also produces the initial flux required in the machine. (MathWorks, n.d.)

5. Switching control block limits the inverter commutation frequency specified value. (MathWorks, n.d.)

6. The magnetization control block is responsible for the switching between magnetization and normal operation modes. (MathWorks, n.d.)

The below Fig 3.4 shows the input parameters set in the DTC/DTFC block.

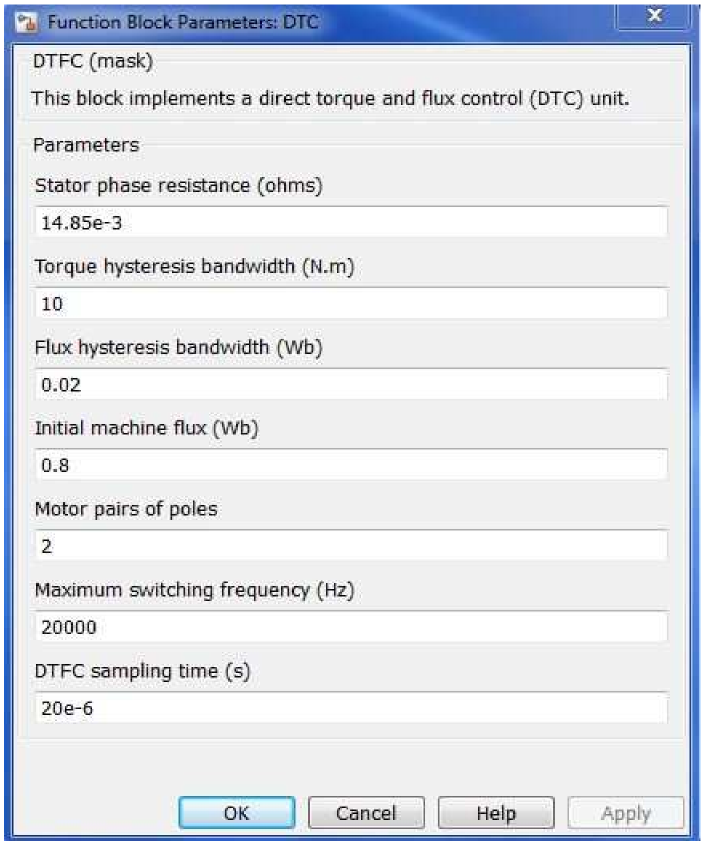

Fig. 3.4 Block parameters for DTC/DTFC block.

<u>Speed Controller Block:</u>

The speed controller block is used in vector-controlled drives. A current motor speed is fed to the speed controller that is used in conjunction with the reference speed to generate an error speed. That error speed is used as an input to a PI controller for speed regulation.

Fig. 3.5 shows the speed controller block.

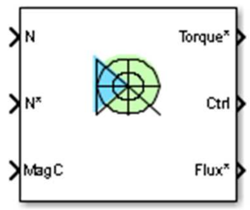

Fig. 3.5 Speed controller block.

The ports N, N*, and MagC serve as the input ports and Torque*, Ctrl and Flux* ports are the output ports.

N is the speed of the induction machine rotor in rpm; N* is the reference speed provided to the induction motor in rpm. Like in DTC controller block, MagC is a binary signal indicator which decides if the machine is enough magnetized to start or not. This signal is provided by the DTC controller (MathWorks, n.d.).

Reference torque, the PI control output, is provided by this block. The flux reference is also calculated using a speed/flux reference table in the block. From the Ctrl port, we can acquire torque reference, flux reference, error and speed reference.

Fig. 3.6 shows the layers in the speed controller block (MathWorks, MathWorks, n.d.).

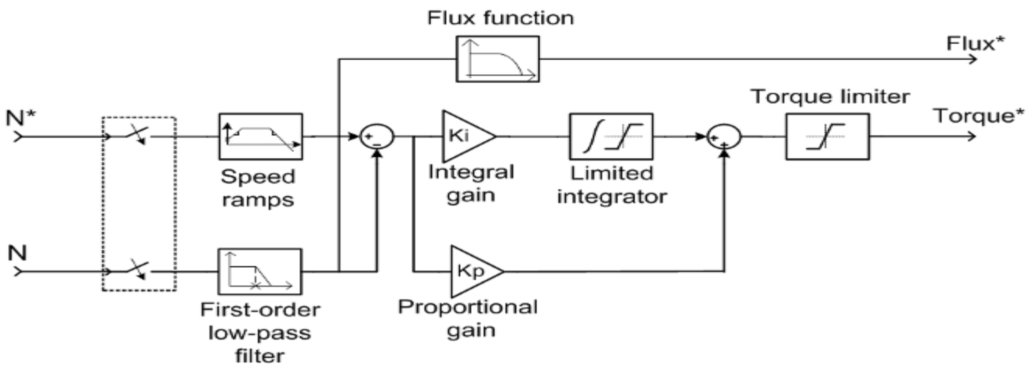

Fig. 3.6. Speed controller with torque and flux references outputs.

Below, Fig. 3.7 shows the input parameters used for the speed controller.

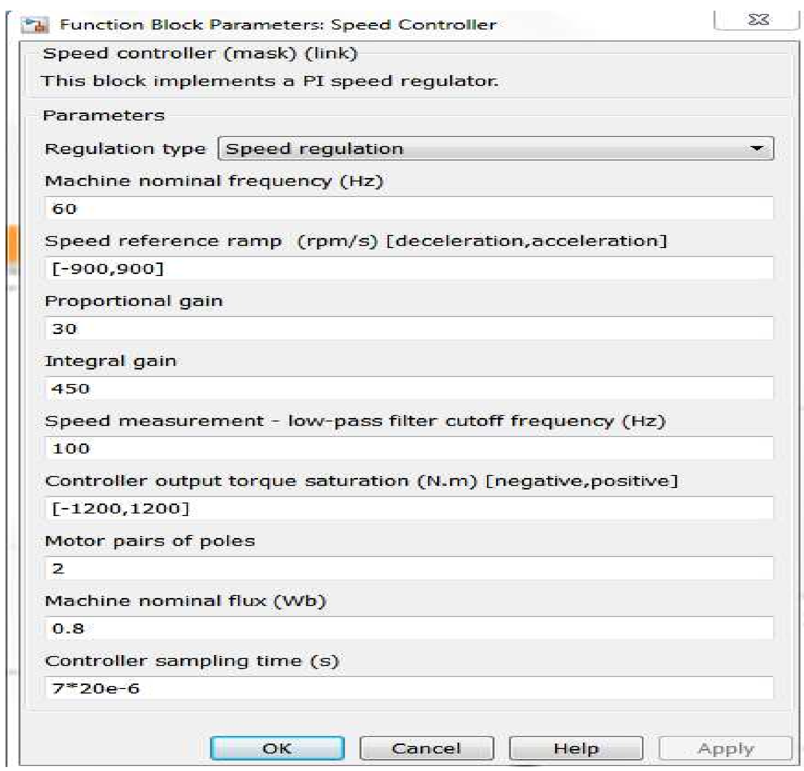

Fig. 3.7 Block parameters for speed controller block.

CHAPTER 4

PROPOSED MODEL FOR SLIP SPEED MEASUREMENT

The proposed model for the slip measurement is based on the direct torque control of the induction motor. The Fig. 4.1 shows the block diagram of the proposed model.

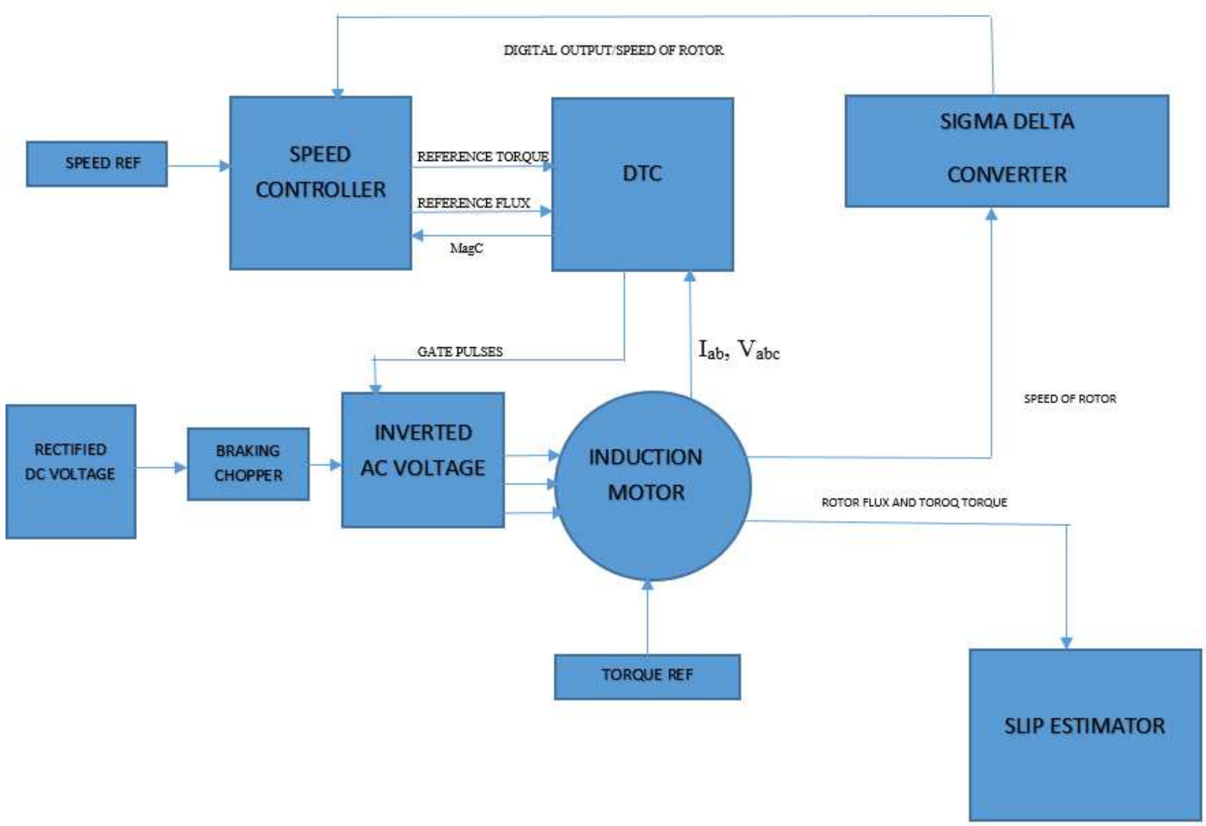

Fig. 4.1 Block diagram of proposed model

From the block diagram, we can observe that the induction machine is fed with an inverted AC supply. A reference speed is given to the speed controller and a torque command is given to the induction motor.

The speed of the rotor is essentially in rad/sec, but the speed controller requires the speed of the rotor to be in rpm so as to compare the actual speed with the reference speed to generate an error that is used in speed regulation. Hence, the rotor speed in rad/sec is converted to rpm.

The direct torque controller is fed with the reference torque and reference speed from the speed controller. The line currents I_{ab} and voltages V_{abc} of the motor are also fed to the torque controller. Now, the DTC analyzes the inputs, processes them and gives the gate pulses as output, which are fed to the inverter for switching process to take place in the inverter.

Fig. 4.2, shows the actual circuit used in this thesis in Matlab.

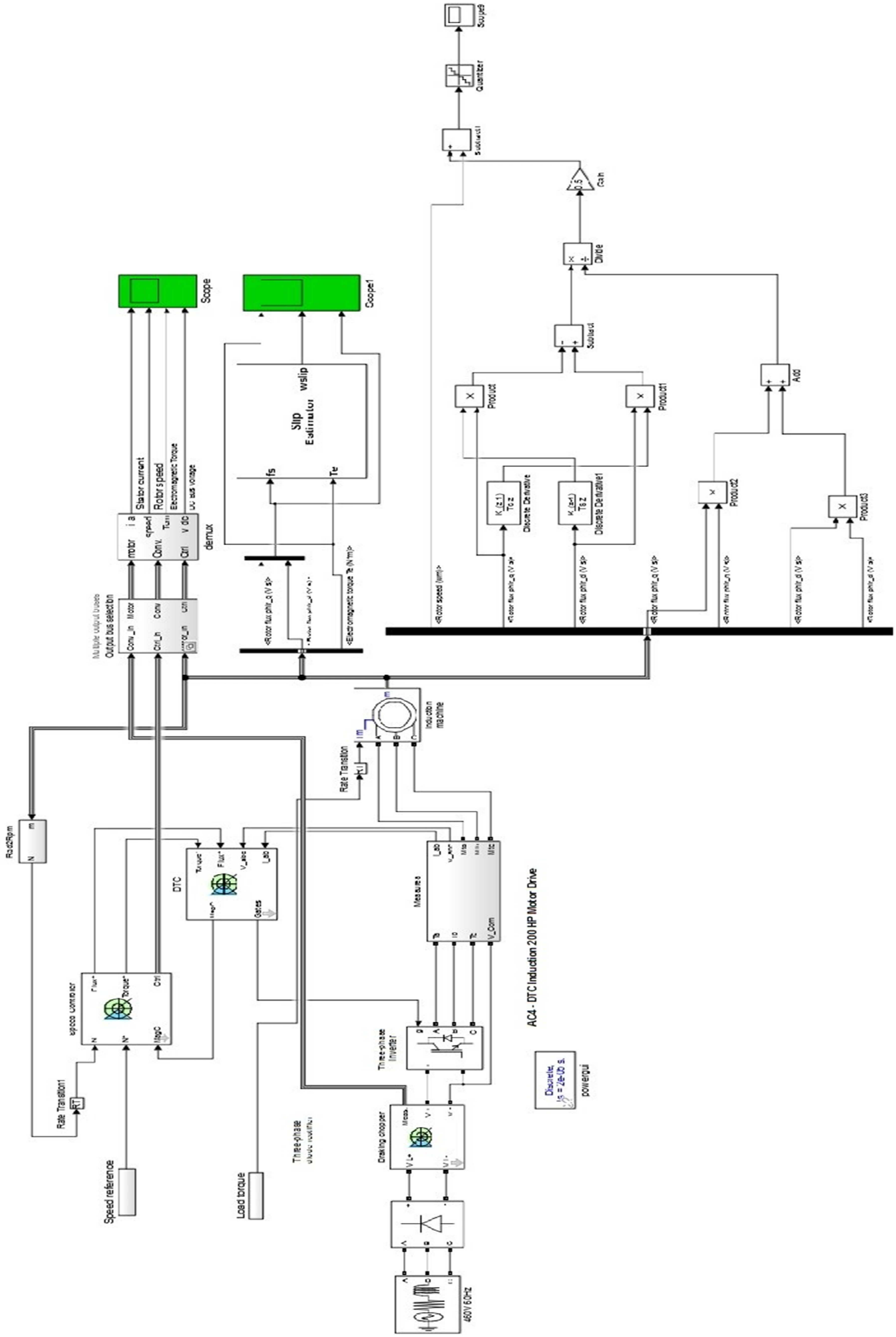

Fig. 4.2. Actual circuit of proposed model

Inputs to the System:

(a) Input supply to the system.

(b) Reference speed command.

(c) Reference torque command.

Input supply to the system.

The three-phase inverter of the DTC scheme is fed by a DC voltage from a three-phase diode rectifier. There is a capacitor used at the output of the rectifier that alters the DC bus voltage ripples, if any. A braking chopper has been added between the rectifier and the inverter to limit the DC bus voltage in case the machine acts as a generator. The below Fig 4.3 shows input supply to the DTC system.

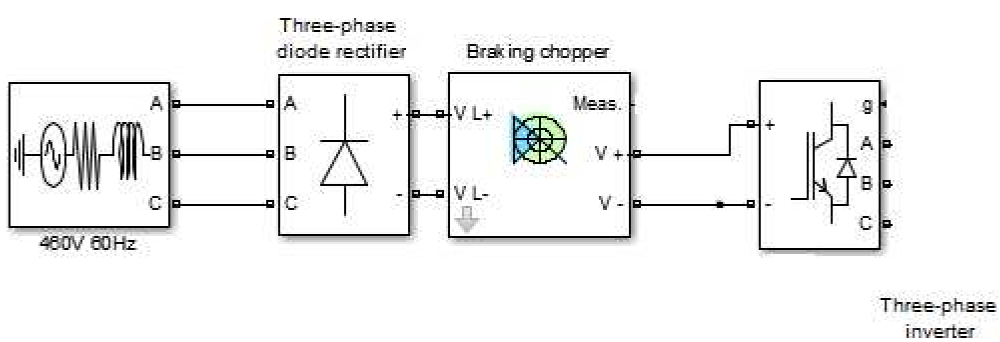

Fig. 4.3 Input supply to the DTC system.

<u>Source AC Voltage:</u>

The source voltage is typically a three-phase, 460V, 60 Hz supply. The three-phase voltage source is in series with a RL branch. The voltage source is connected in "Y" with a neutral connection which can be internally grounded. The source internal resistance and inductance can be manually specified either directly by entering R and L values in the block parameters or by the X/R ratio. Below Fig 4.4 shows source AC voltage.

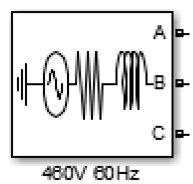

Fig. 4.4 AC supply with RL branch in series.

Below is the formula (4.1) with which internal resistance R is computed from the source reactance X by X/R ratio.

$$R = \left(\frac{X}{\frac{X}{R}}\right) = \frac{2\pi f L}{\frac{X}{R}} \quad (4.1)$$

When explained, f is the specified input frequency of the supply, L is the inductance of the machine.

Below Fig. 4.5 gives the block parameters of the source voltage.

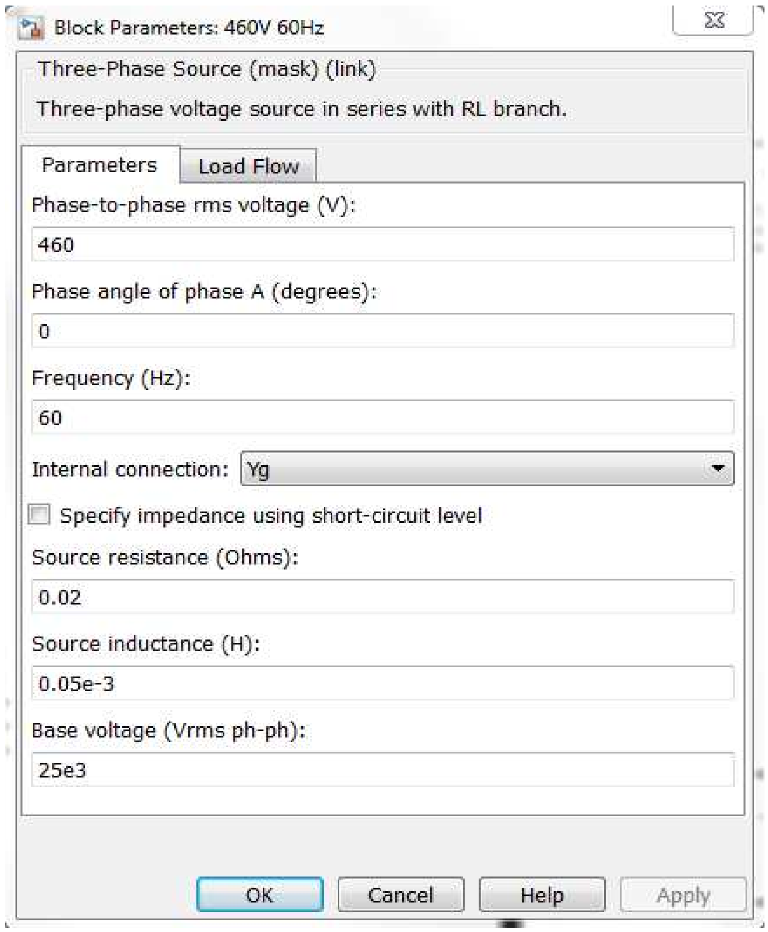

Fig. 4.5 Input supply to DTC system.

<u>Three-Phase Rectifier:</u>

A three-phase rectifier is used to rectify the three-phase AC supply. A capacitor is added at the output of the rectifier so that it alters the DC bus voltage ripples.

Below Fig.4.6 shows the three-phase rectifier used.

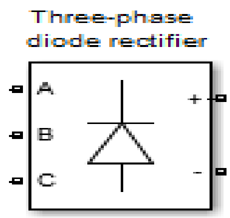

Fig. 4.6 Three-phase rectifier.

Below Fig. 4.7 gives the block parameters of the three-phase rectifier.

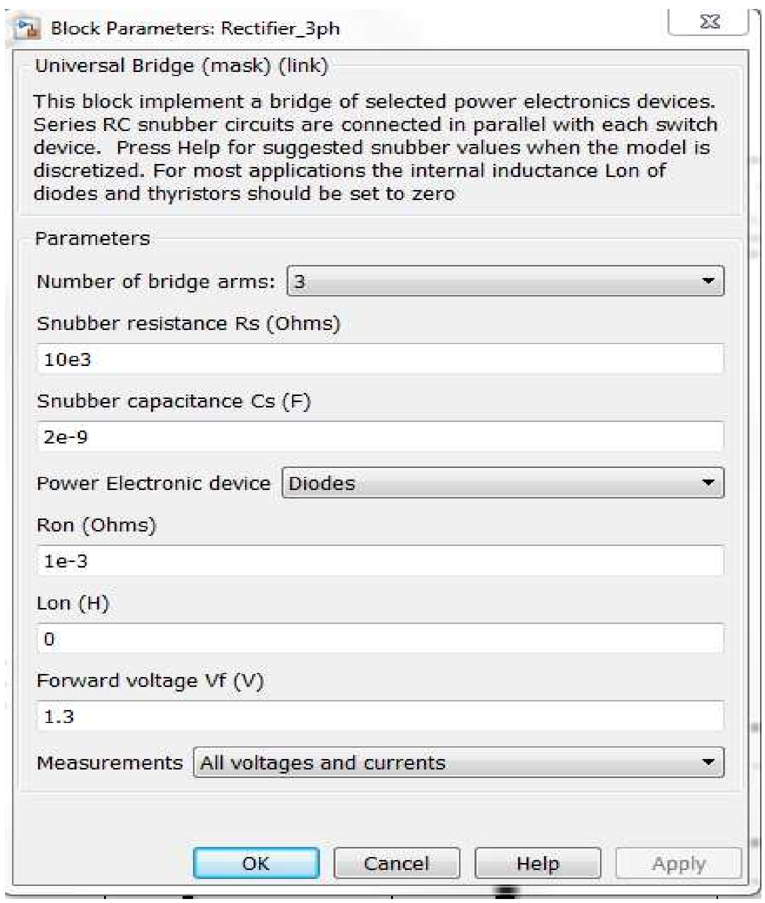

Fig. 4.7 Block parameters of three-phase rectifier.

<u>Braking Chopper:</u>

As observed from the circuit, there is an AC voltage supply to the rectifier which rectifies the AC supply to DC and then a braking chopper is placed in between the rectifier and the inverter.

The main purpose of the braking chopper is that it controls the voltage when the energy is fed back to the intermediate circuit from the load. For example, this scenario arises when a magnetized motor, which is being rotated by an overhauling load and feeding power to the DC voltage intermediate circuit, functions as a generator.

Hence, by using the braking chopper, the DC bus voltage is limited by switching the braking energy to a resistor where it is converted to heat. The braking chopper gets automatically activated at the time where the voltage at the DC bus exceeds a pre-specified level considering the nominal voltage of the VFD (variable frequency drive). Fig. 4.8 below shows the braking chopper block.

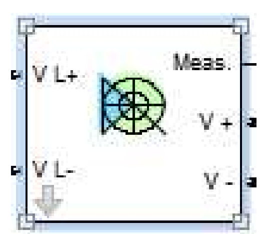

Fig. 4.8 Braking chopper block.

As seen in the above figure, the braking chopper has two inputs and three output ports. The VL+ and VL- ports serve as the input ports from which the output of the rectifier, which is essentially a DC supply, is fed to the chopper.

As the motor is magnetized, when in case the motor acts as a generator, the chopper limits the bus voltage by burning the energy through a resistor.

The outputs of the braking chopper V+ and V- are connected to the input terminals of the three-phase inverter. From Meas terminal (measurement port) we can measure V_{bus}, $I_{rectified}$, and I_{bus}. Below Fig 4.9 shows the block parameters of the braking chopper.

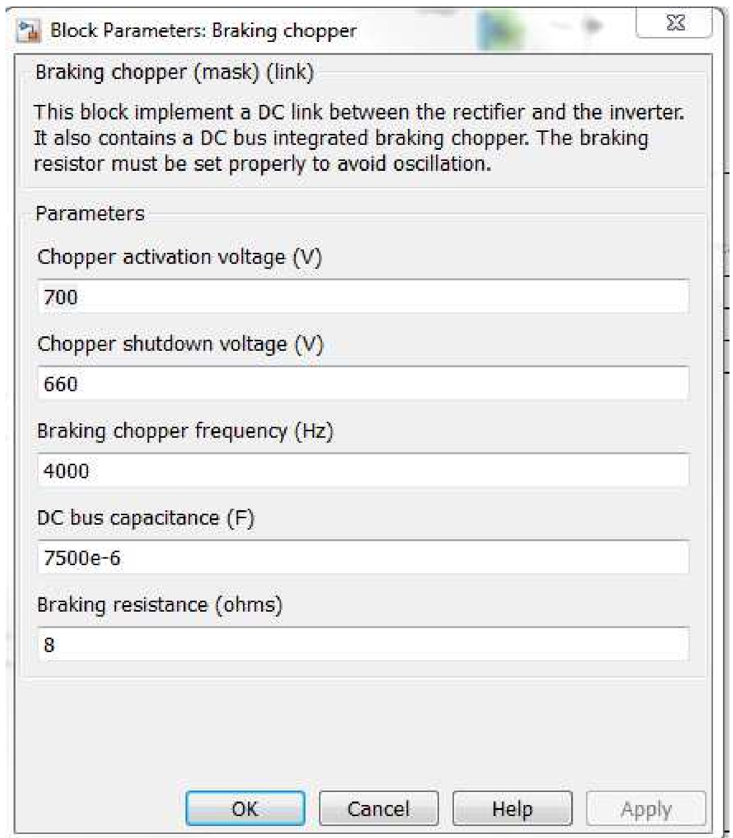

Fig. 4.9 Block parameters of braking chopper.

<u>Three-Phase Inverter:</u>

The output from the braking chopper is connected to the three-phase inverter. The output of the inverter is a three-phase AC voltage which is fed to the induction motor.

The inverter is triggered with the gate pulse signals from the DTC controller block as seen in Fig.4.8. Below is Fig 4.10 showing three-phase inverter.

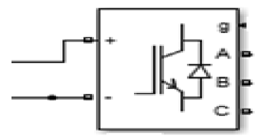

Fig. 4.10 Three-phase inverter.

Below is Fig 4.11 showing block parameters of the inverter.

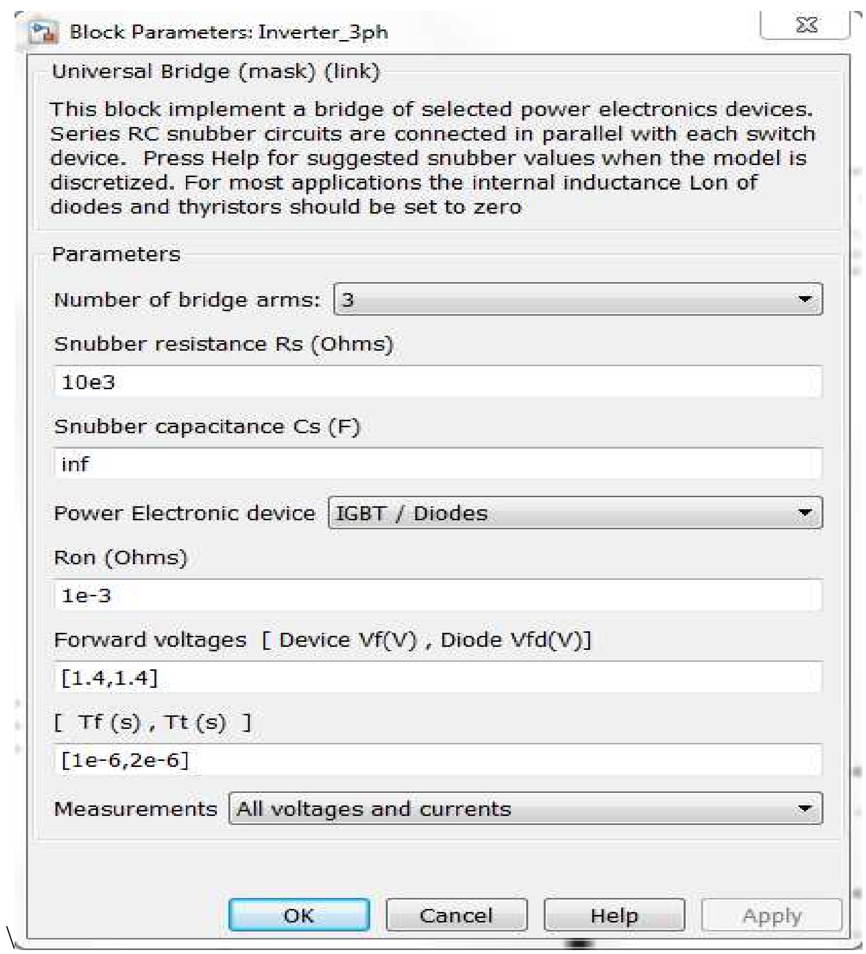

Fig. 4.11 Block parameters of three-phase inverter.

Additionally, a measuring block is placed between the inverter and the induction machine to measure the currents Ia, Ib and Voltages V_abc. The measurement block uses current measurement and voltage measurement blocks to measure the current and voltages respectively as seen in Fig 4.12.

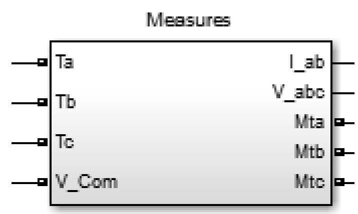

Fig. 4.12 Measures block.

The below Fig. 4.13 shows the layers in the measuring block.

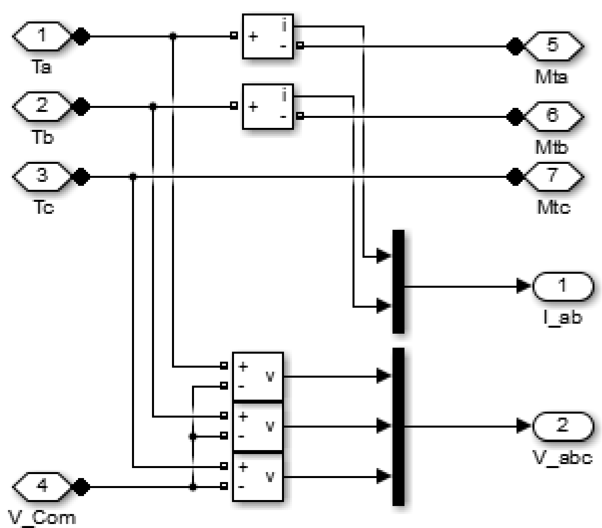

Fig. 4.13 Layers in the measurement block for I and V measurement.

Induction Motor:

A three-phase asynchronous machine is adopted from the Simulink library. It can operate in generator or motor mode. Its mode of operation is based on the mechanical torque. The machine runs as a motor if Tm is positive. If Tm is negative, the machine is a generator. As we want the mode of the machine to be a motor, Tm is desired to be positive as in Fig. 4.14.

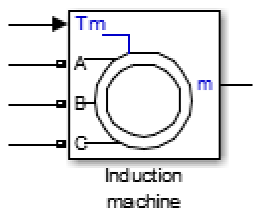

Fig. 4.14 Induction machine.

The output of the induction motor can be connected to a bus to measure different values of the induction motor course its operation. They are:

(i) Stator measurements

(ii) Rotor measurements

(iii) Mechanical measurements

(iv) Lm (H)

Stator measurements include:

Stator current is_a (A)

Stator current is_b (A)

Stator current is_c (A)

Stator current is_q (A)

Stator current is_d (A)

Stator flux phis_q (V_s)

Stator flux phis_d (V_s)

Stator voltage vs_q (V)

Stator voltage vs_d (V)

<u>Rotor measurements include:</u>

Rotor current ir_a (A)

Rotor current ir_b (A)

Rotor current ir_c (A)

Rotor current iq (A)

Rotor current id (A)

Rotor flux phir_q (V_s)

Rotor flux phir_d (V_s)

Rotor voltage vr_q (V)

Rotor voltage vr_d (V)

<u>Mechanical measurements include:</u>

Rotor speed (wm)

Electromagnetic torque Te (N*m)

Rotor angle theta m (rad)

Lm (H) is the inductance of the machine.

These values are used to calculate the slip frequency of the motor.

The block configuration and parameters of the induction machine are shown below in Figures 4.15 and 4.16 respectively.

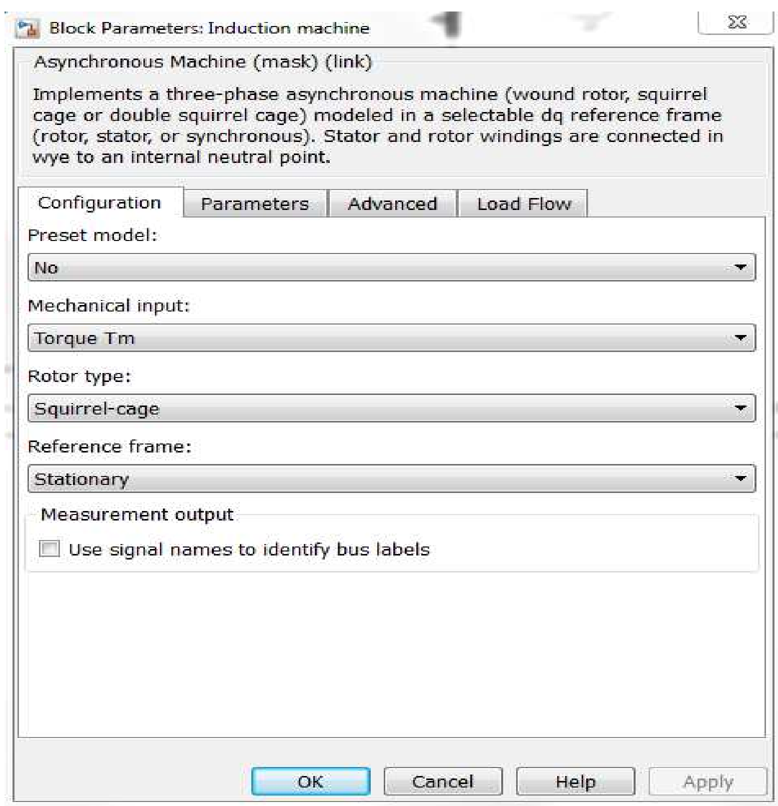

Fig. 4.15 Block configuration of induction machine.

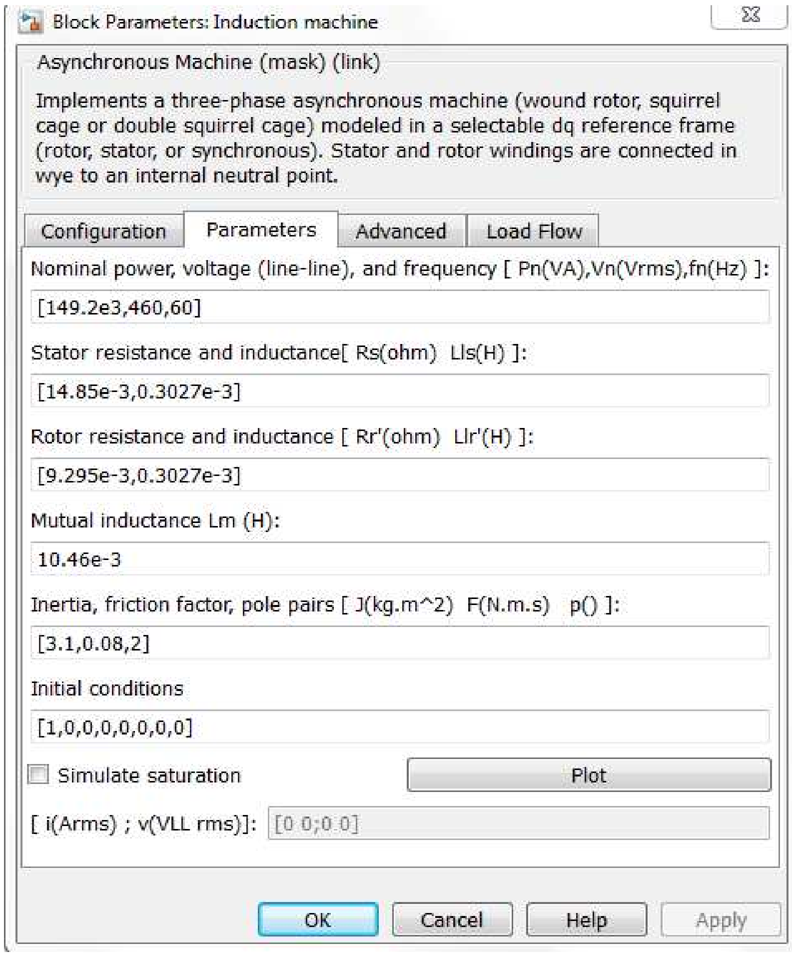

Fig. 4.16 Block parameters of the induction machine.

CHAPTER 5

SLIP MEASUREMENT

The heart of this thesis is measuring the slip frequency of the induction motor. Thus, two techniques were developed to measure the slip frequency:

1. Slip frequency measurement using electrical torque equation.
2. Slip frequency calculation using the rotor flux voltages and their derivatives.

Slip Frequency Measurement Using Electrical Torque Equation:

The torque equation of an induction machine is noted to be

$$T_e = \left[\frac{3}{2} p \frac{{L_r}^2}{R_r {L_s}^2} |\varphi_s|^2\right] \omega_{slip} \tag{5.1}$$

here, T_e is the electrical torque

P is number of poles

L_r is the stator inductance

L_s is the rotor inductance

ω_{slip} is the slip frequency

φ_s is the stator flux

The above equation 5.1 can be manipulated to get the slip frequency as

$$\omega_{slip} = \frac{T_e}{|\varphi_s|^2}\frac{2R_r}{3p}\frac{{L_s}^2}{{L_r}^2} \tag{5.2}$$

From Fig. 4.16, we can observe that the stator inductance and the rotor inductance of the induction motor are equal to be 0.3027e-3 H. Thus the equation changes to

$$\omega_{slip} = \frac{T_e}{|\varphi_s|^2}\frac{2R_r}{3p} \tag{5.3}$$

The above equation. 5.3 is used to calculate the slip frequency.

A slip estimator is built in Simulink using the above equation. The schematic of the slip estimator is shown below in Fig. 5.1.

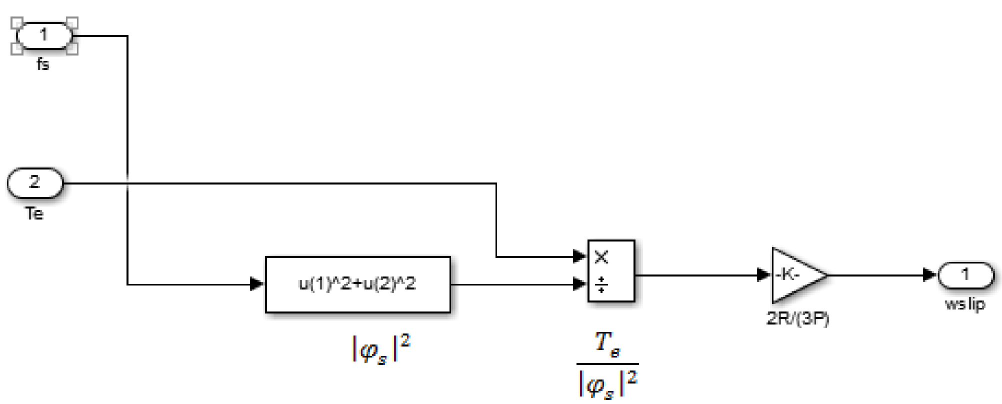

Fig. 5.1 Slip estimator.

<u>Slip Frequency Calculation Using the Rotor Flux Voltages and Their Derivatives:</u>

A method of determining the frequency more continuously is discussed here. The basic frequency detection scheme requires two orthogonal waveforms and their derivatives to do the calculations. Since both flux, its derivative and the flux voltages can be extracted from the output bus of the induction motor, this method would be simple to implement.

The frequency detection scheme is shown in the below Fig. 5.2.

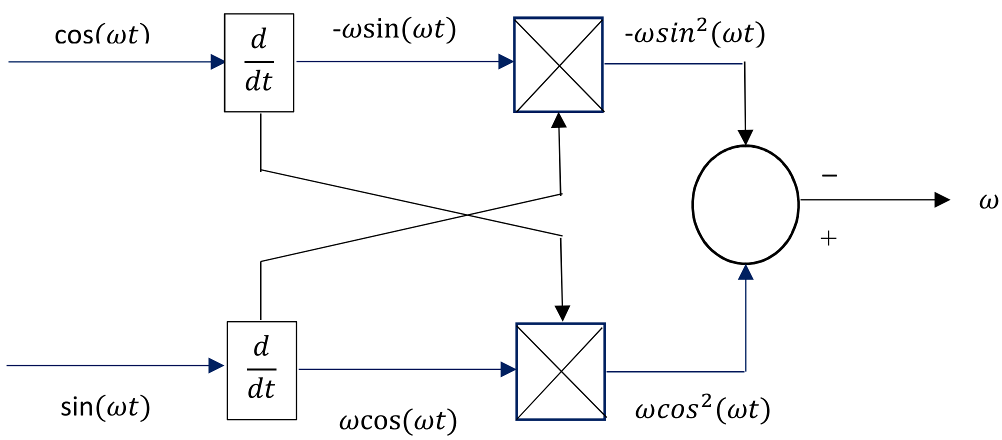

Fig. 5.2 Frequency detection scheme using sine and cosine waveforms and their derivatives.

As the rotor flux and the rotor flux voltages extracted from the induction machine are dq transformed, the above system could be implemented in dq coordinates (Fig. 5.3).

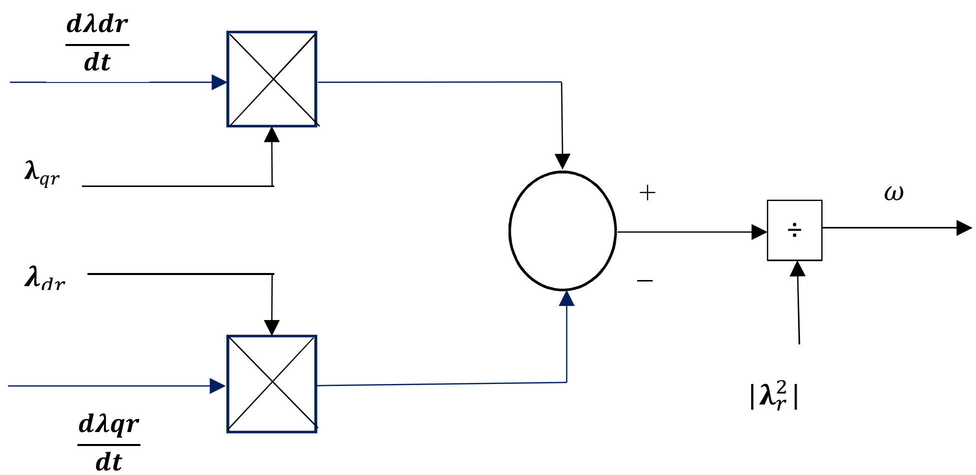

Fig. 5.3 Frequency detection using flux and flux voltage in dq coordinates.

Below Fig. 5.4 shows the frequency detection using flux derivatives and flux voltages in Simulink.

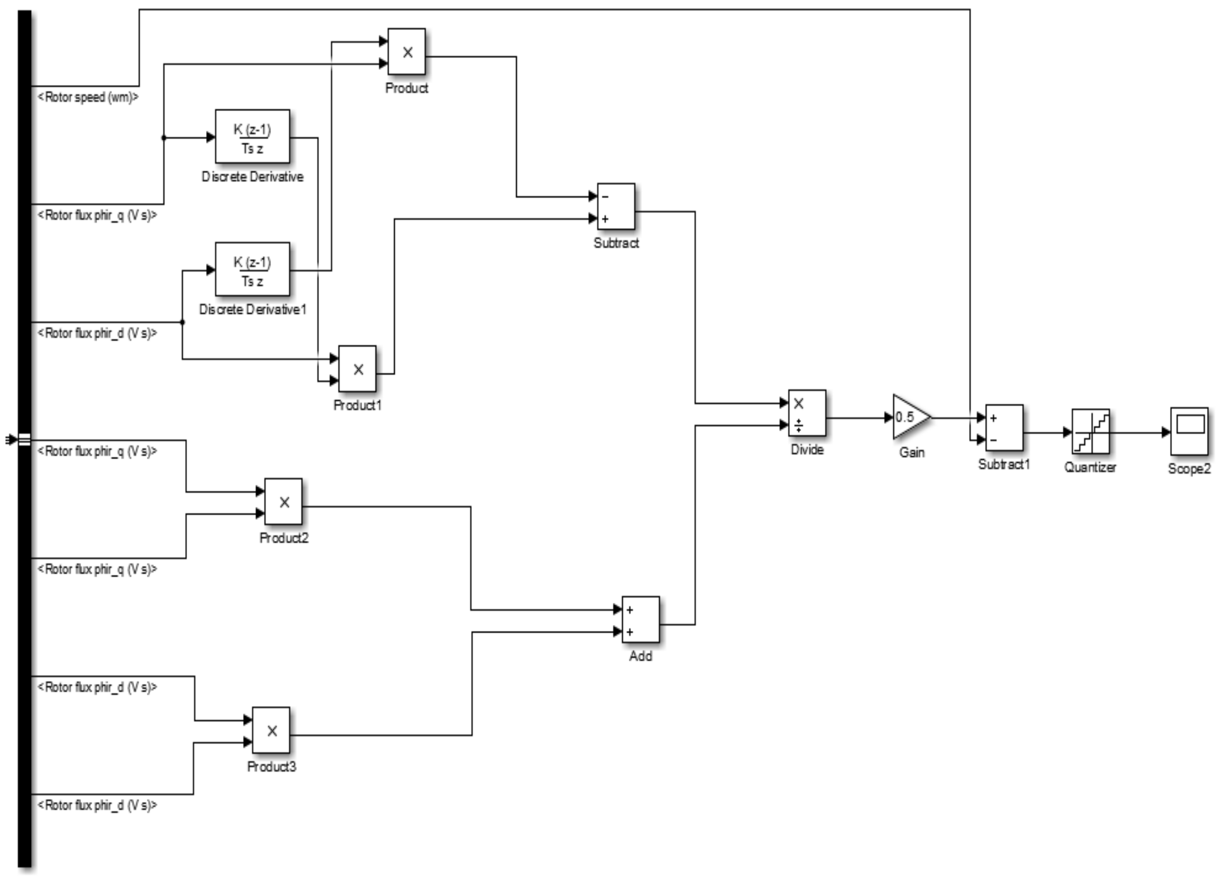

Fig. 5.4 frequency detection using flux derivatives and flux voltages in Matlab.

Here for the frequency detection using flux derivatives and flux voltages, both the d and q components of the rotor flux and the voltages are used.

The derivative of q component of the rotor flux voltage is multiplied with the d component of the rotor flux voltage.

The derivative of d component of the rotor flux voltage is multiplied with the q component of the rotor flux voltage. The difference between the two products is divided by the square of the rotor fluxes. The resultant is the electrical frequency.

The electrical speed of the machine is calculated by dividing the electrical frequency by the number of pole pairs. The relation can be explained as

$$Ns = \frac{\omega f}{\text{pole pairs}} \tag{5.4}$$

Our induction motor had two pole pairs, thus the equation becomes

$$Ns = \frac{\omega f}{2} \tag{5.5}$$

The synchronous speed of the motor is calculated using the above equation which is in rad/sec.

As discussed, the slip is the difference between synchronous speed and the actual speed of the rotor (Manney, 2013). The rotor speed can be obtained from the output bus of the induction motor which is in rad/sec.

Taking the difference of Ns and Nr gives us the slip of the motor, which is nothing but

$$S = Ns - Nr \tag{5.6}$$

<u>Comparison of Both the Techniques Used:</u>

Let's compare both the techniques used to calculate the slip frequency. Here while calculating slip frequency using electrical torque equation,

$$\omega_{slip} = \frac{T_e}{|\varphi_s|^2}\frac{2R_r}{3p} \qquad (5.3)$$

The slip frequency is directly proportional to the rotor frequency Rr.

While the motor is operating, the rotor windings get heated up and the resistance values may change. The resulting change in slip frequency may not be desired value.

On the other hand, while calculating the slip frequency using flux derivatives and flux voltages, the electrical frequency is completely based on the rotor flux values which do not change with temperature rise. Even though the calculation part is tricky, the slip frequency values are accurate at any instant.

CHAPTER 6

SIMULATIONS AND RESULTS

The circuit is rigged and simulated in Matlab R2015A. All the blocks used in the circuit are available in the Simulink library of the software.

The sample time Ts of the model is chosen to be Ts = 20 ms.

From equation 2.1, the no-load speed of the induction machine is its synchronous speed, which is

$$Ns = 120*f/P$$

here, for this example, f = 60 Hz, P = 4, making

$$Ns = 1800 \text{ rpm}$$

The rated torque of the machine is

$$T = \frac{POWER\ in\ Watts}{SPEED\ (rad/sec)} \tag{6.1}$$

For this example,

Power in Watts = 149.2×10^3 Watts

Speed in rad/sec = 188.4 rad/sec

Torque (T) = 791.9 N-m

The amplitude of speed reference to the speed controller is 750 at 0 sec and 1000 at 1 sec as seen in Fig. 6.1.

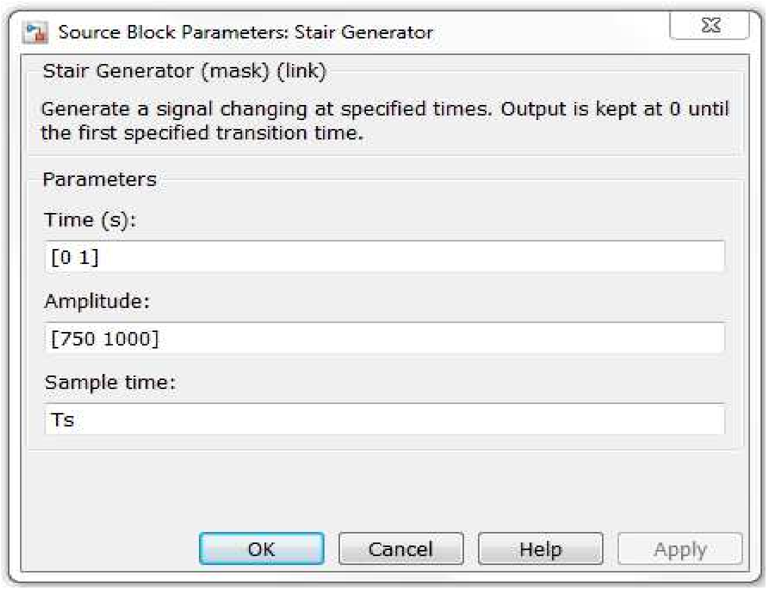

Fig. 6.1 Speed reference to speed control.

The reference torque command to the induction machine is 0 at 0 sec and 791 at 2 secs as seen in Fig. 6.2.

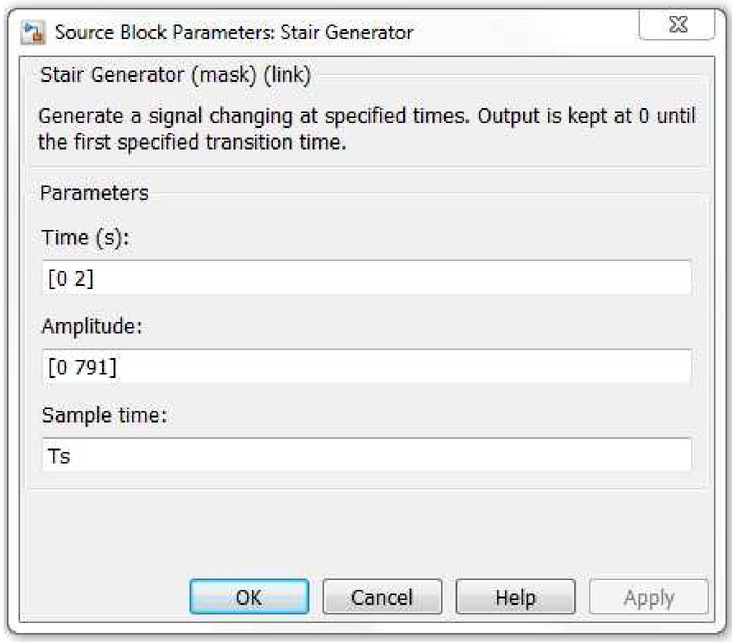

Fig. 6.2 Torque command to induction motor.

The speed input to the speed controller should be rpm. So the speed of the rotor, which is in rad/sec, is converted to rpm. Below Fig. 6.3 shows the signals before and after conversion.

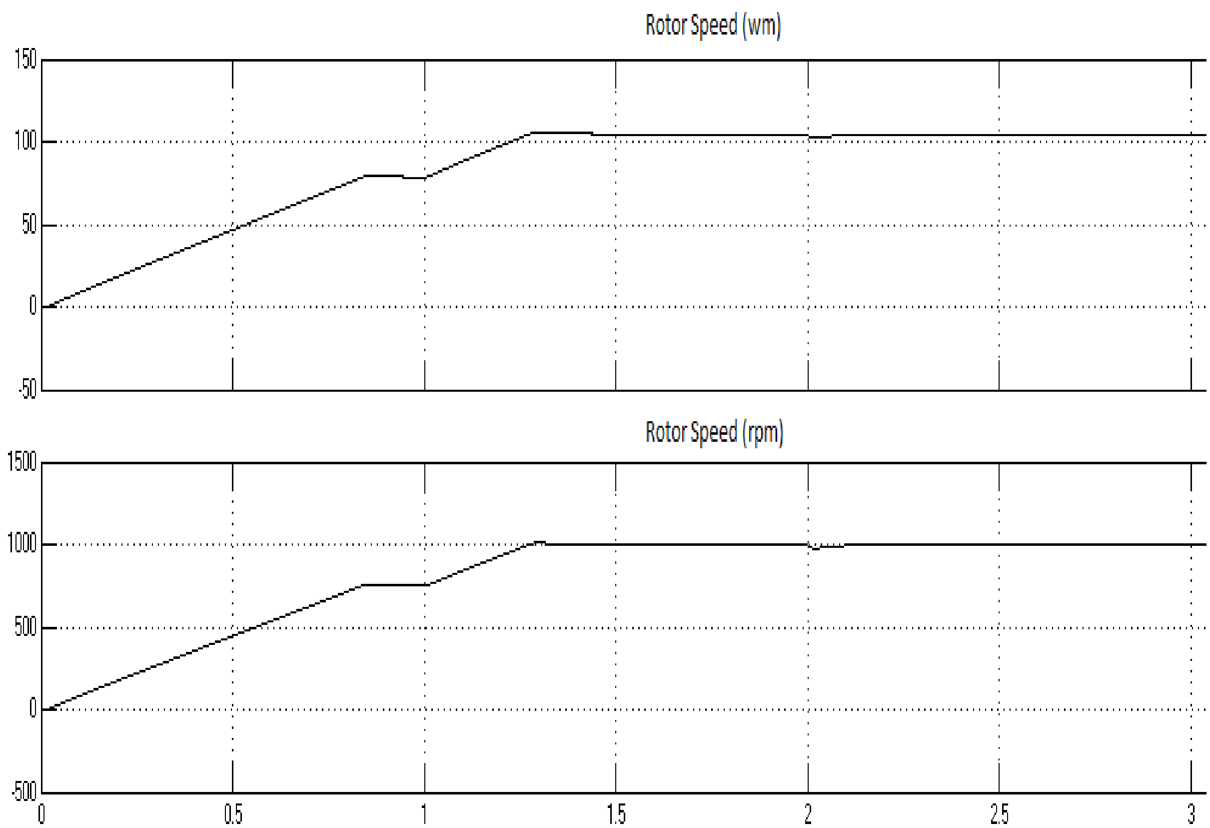

Fig. 6.3 Speed in rad/sec and rpm

Below Fig. 6.4 shows the rotor flux with dq components.

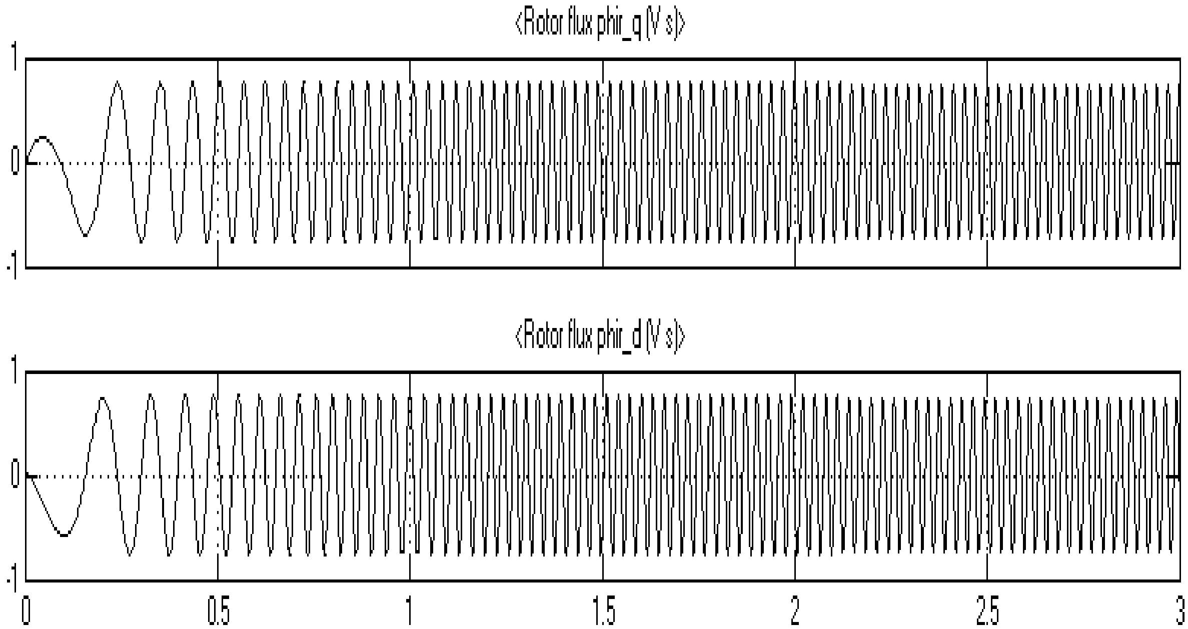

Fig. 6.4 Rotor flux with q component and d component.

From the plot, it can be observed that both the components have the same magnitude but are 90 degrees out of phase.

The below Fig. 6.5 shows the stator current of the induction motor.

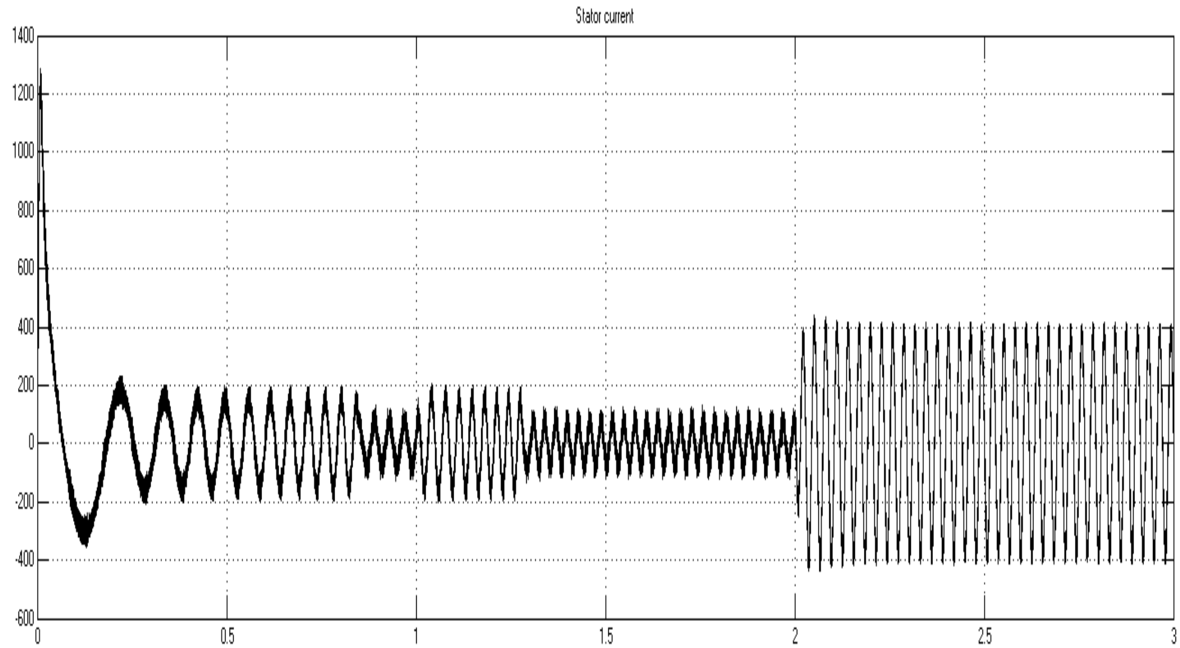

Fig. 6.5 Stator current of the induction motor.

The magnitude of the stator current is around 200A from 1 to 1.25 secs. It drops down to around 180A from 1.25secs to 2 sec. At 2 secs when the motor attains steady state, the stator current increases to 400A and stays constant.

Fig. 6.6 shows the DC bus voltage.

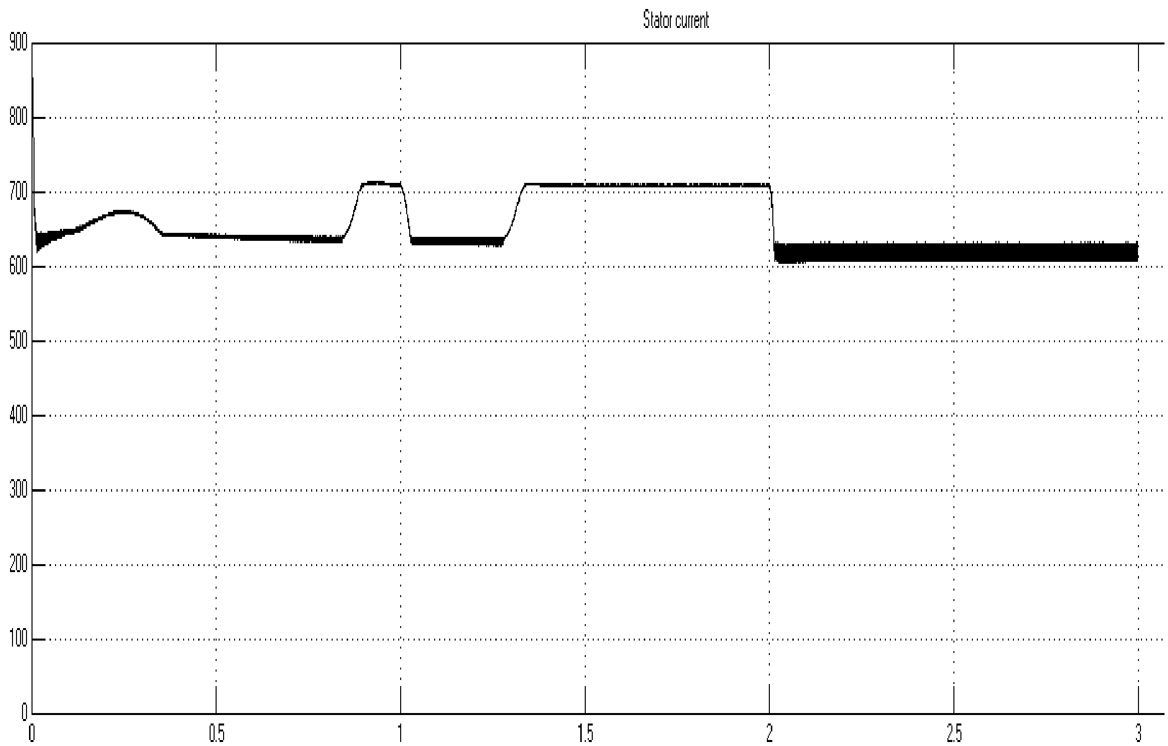

Fig. 6.6 DC bus voltage.

Unlike the stator current, the DC bus voltage has a magnitude of 650V from 1.02secs to 1.28 secs, increases to 700V at 1.38 secs and stays constant until 2 secs, then decreases to 610V and stays constant.

The electromagnetic torque of the motor is shown below in Fig. 6.7.

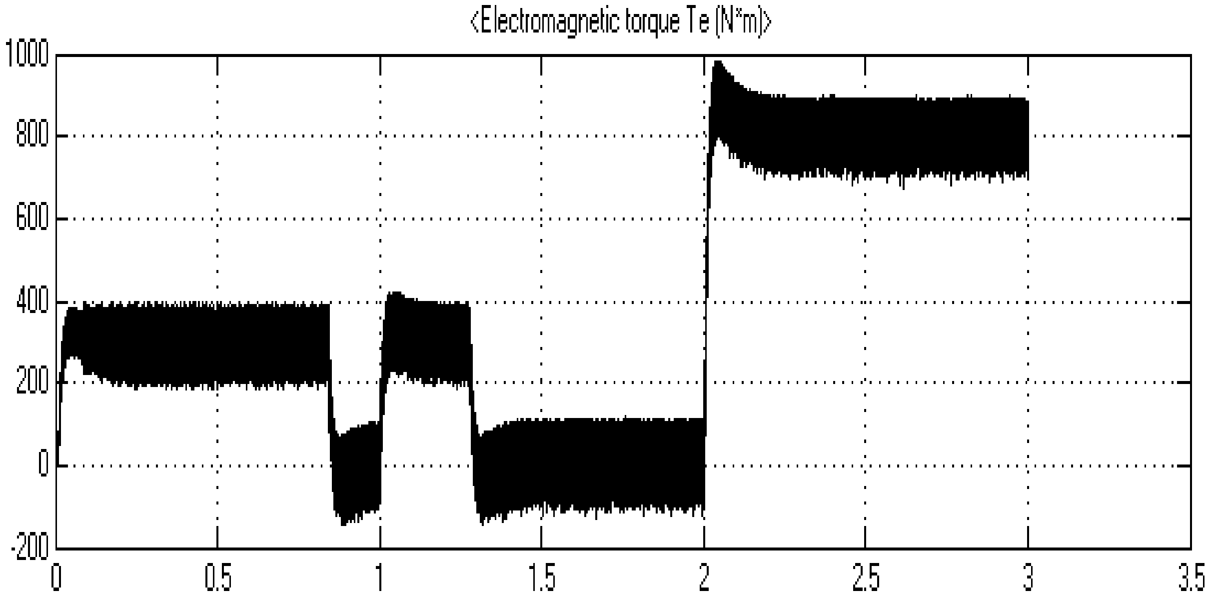

Fig. 6.7 Electromagnetic torque of the motor.

The amplitude of the electromagnetic torque from the machine is around 200 N-m to 400 N-m from o to .8 secs, then drops to 50 N-m and -150 N-m from .8 secs to 1 sec, it increases to the applied torque reference of 791 N-m after the machine achieves steady state.

A comparison of DC bus voltage and electromagnetic torque is shown in Fig. 6.8.

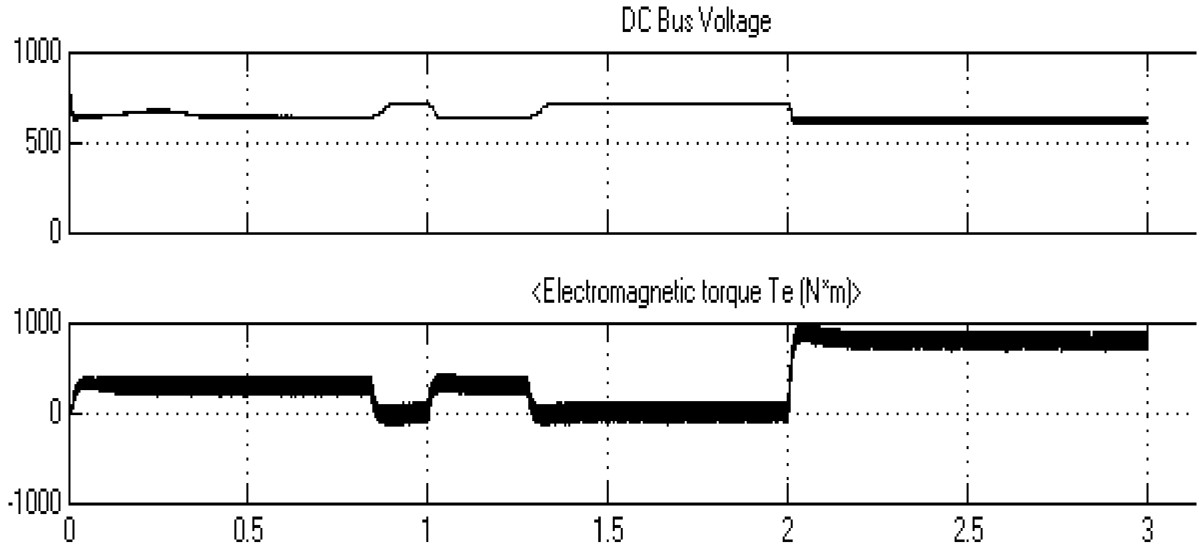

Fig. 6.8 Comparison of DC bus voltage and electromagnetic torque.

Here we can observe that plots of the DC bus voltage and electromagnetic torque display inversely proportional characteristics; i.e., when the voltage decreases the electromagnetic torque of the machine increases and when the voltage increases the electromagnetic torque decreases. Both become constant when the machine achieves a steady state, which is at 2 sec.

Now looking in the slip estimator block, from equation 6.3 the estimation is based on

$$\omega_{slip} = \frac{T_e}{|\varphi_s|^2}\frac{2R_r}{3p} \tag{5.3}$$

Hence, the fluxes are squared to get to get the slip frequency.

Fig. 6.9 gives the plot before and after squaring the fluxes. From the plots of the flux squares, the highest peak of the wave is found to be at 0.599 wb^2.

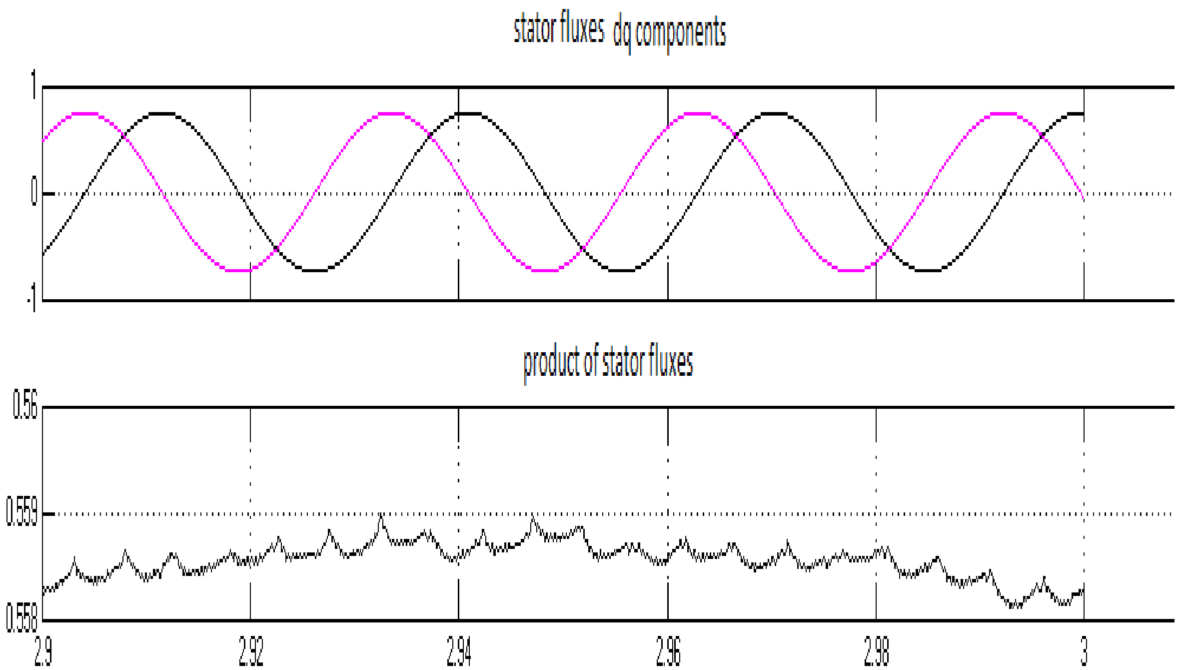

Fig. 6.9 Before and after squaring the fluxes.

The electromagnetic torque / Flux^2 plot is shown below in Fig. 6.10. We observe that at steady state the Te produced has a band from 700 to 900 Nm.

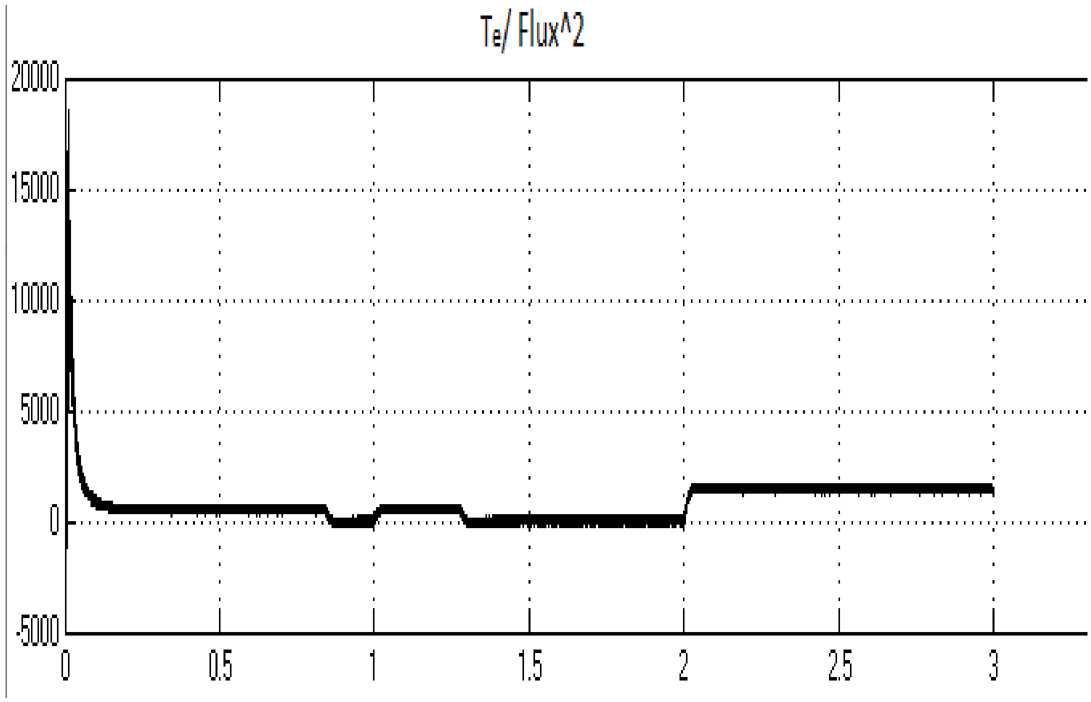

Fig. 6.10 Electromagnetic torque/flux^2.

Continuing the equation, for slip frequency, Te/flux^2 is multiplied with 2Rr/3P, where Rr is the rotor resistance and p is the number of poles. The resultant gives us the flux frequency which is shown in Fig. 6.11.

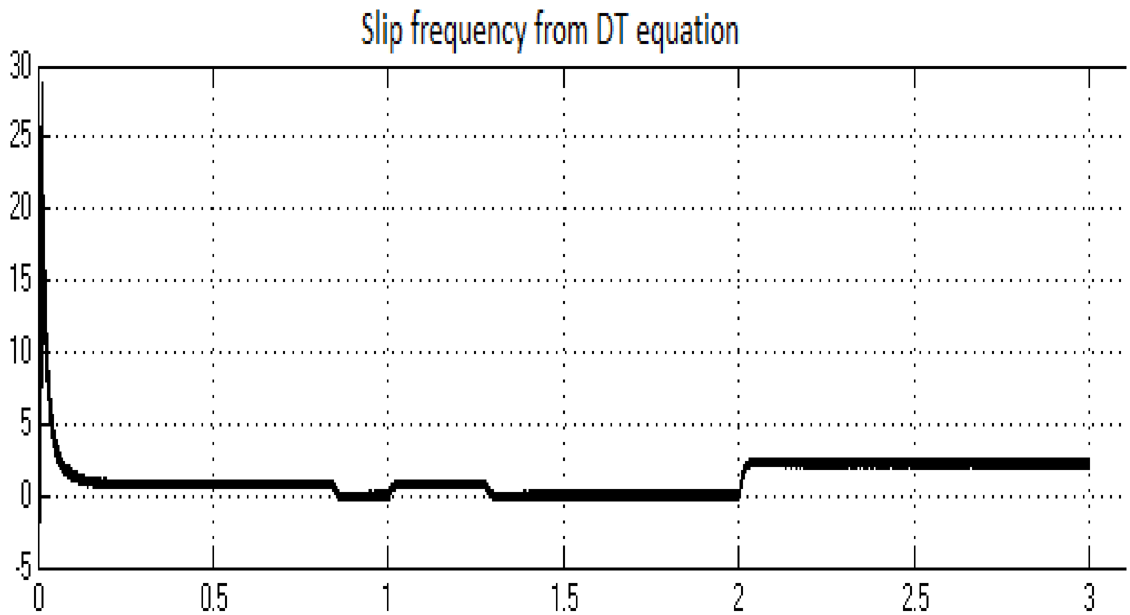

Fig. 6.11 Slip frequency as an output from slip estimator.

The above Fig. 6.11 shows the slip frequency from the slip estimator. When the machine achieves steady state, the slip frequency is measured to be 2.

Considering the inputs and outputs of the slip estimator, from Fig. 6.12, the first two axes in the plot are the electromagnetic torque and flux of the machine, which are the inputs to the slip estimator. The third axis is the slip frequency of the motor.

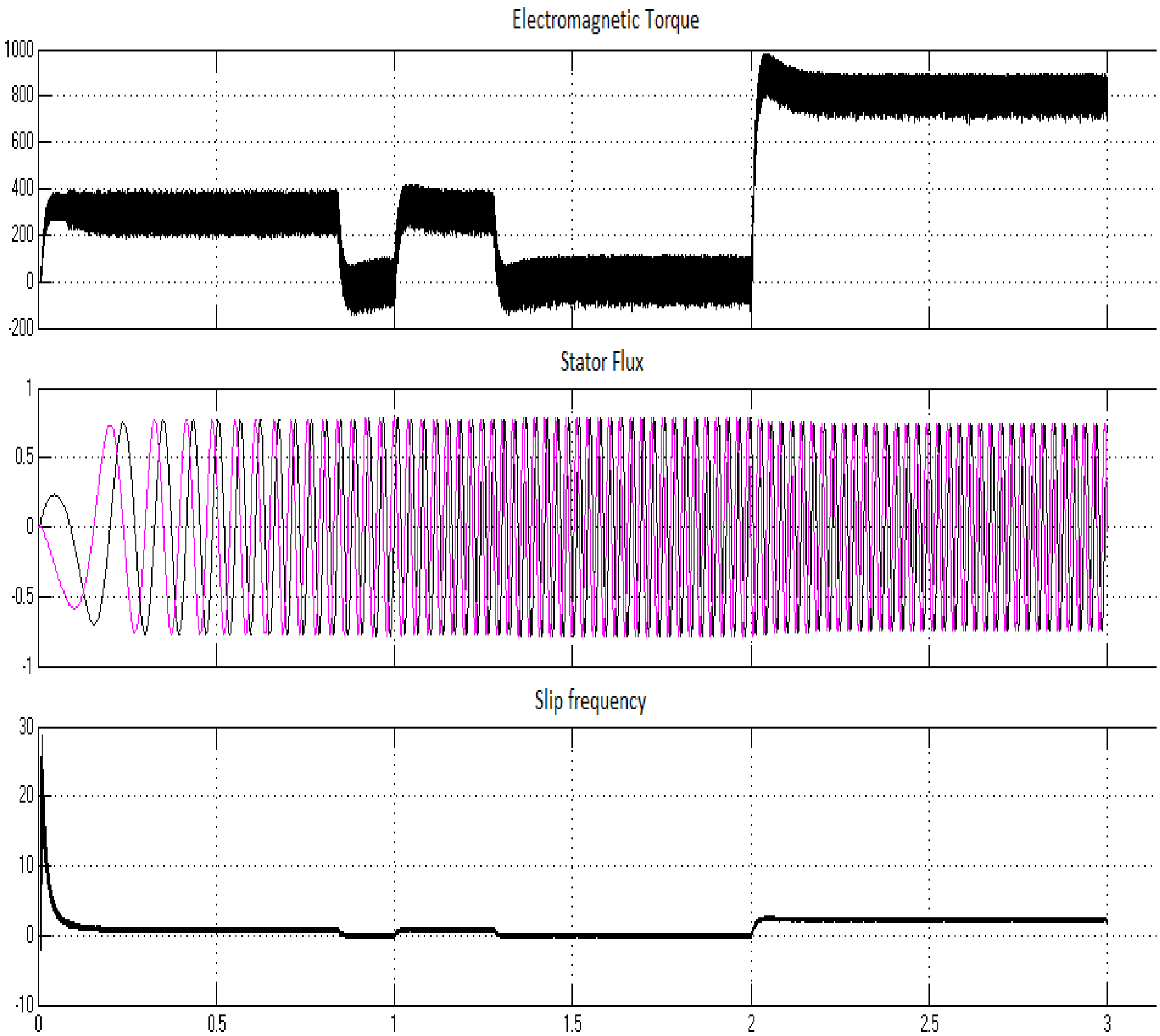

Fig. 6.12 Inputs and outputs of the slip estimator.

Concentrating on the other method to calculate the slip frequency using flux and their derivatives, the dq components of the rotor flux and their derivatives are used to calculate the slip frequency. Let's have a look at the dq components of the fluxes and their derivatives and compare them.

First, we'll compare the q component of the rotor flux and its derivative as shown in Fig. 6.13. The peak value of the q component of the rotor flux is observed to be 0.75Wb and the peak of the derivative of q component is observed to be 180Wb.

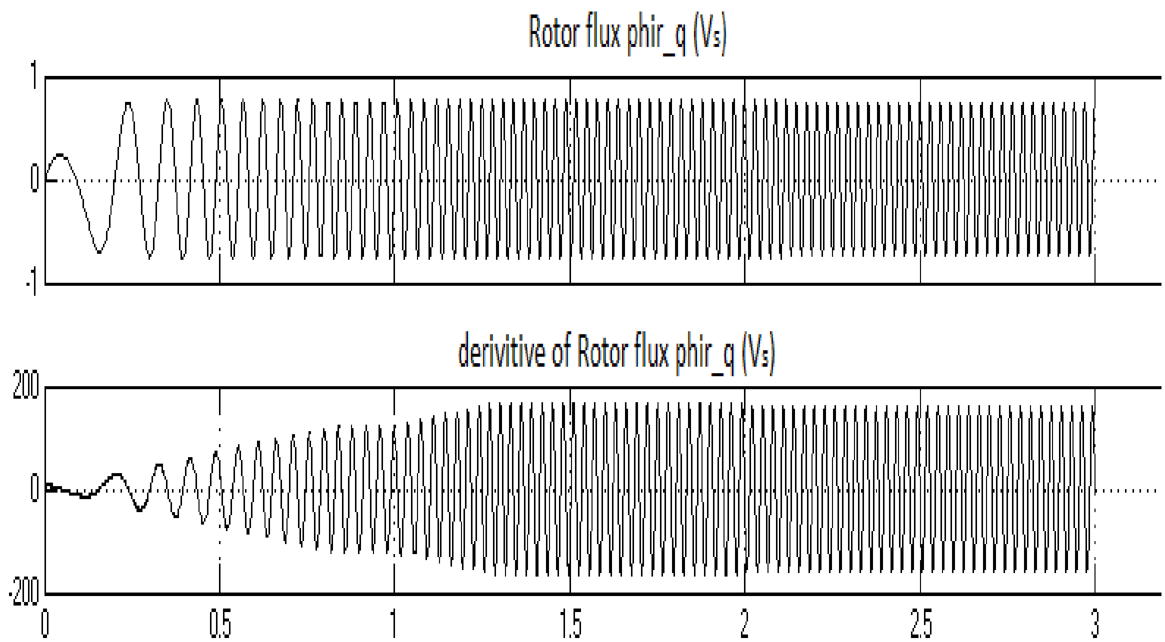

Fig. 6.13 "q" component of rotor flux and its derivative.

Now, comparing the d component of the rotor flux and its derivative as shown in Fig. 6.14, like the peak value of the q component, the d component of the rotor flux is observed to be 0.75Wb and the peak of the derivative of d component is observed to be 180Wb.

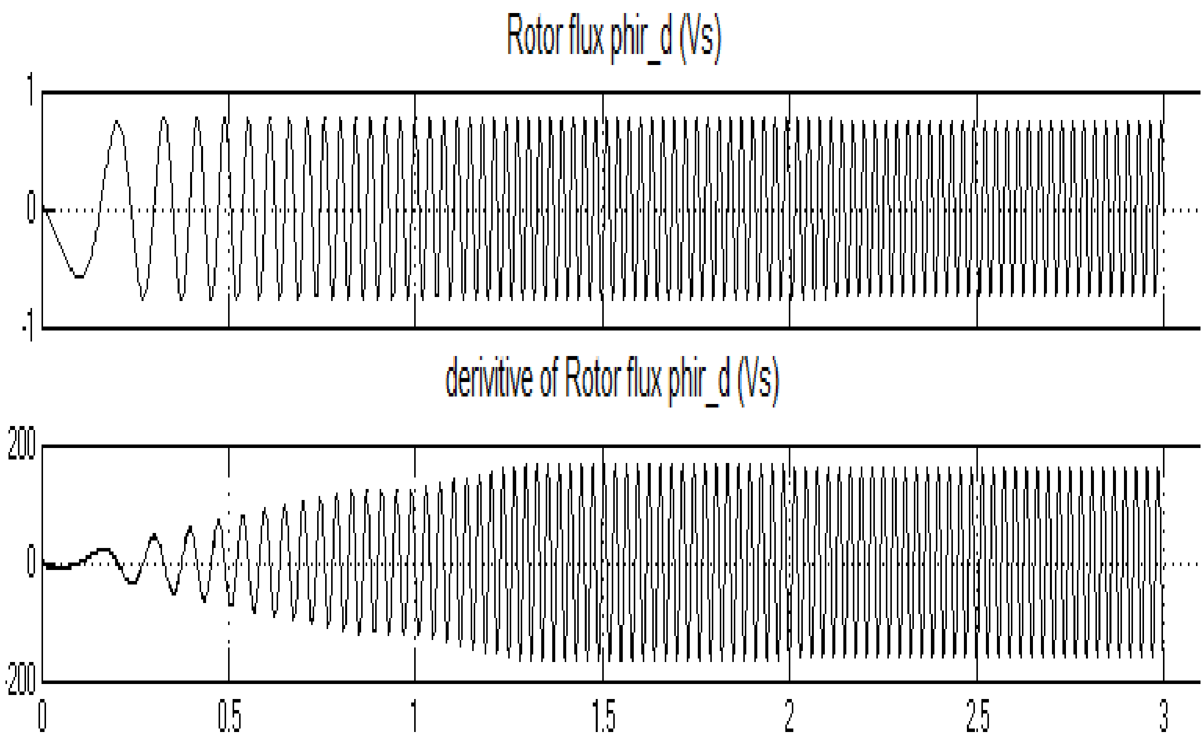

Fig. 6.14 “d” component of the rotor flux and its derivative.

Now the q component of the rotor flux is multiplied with the derivative of the d component of the rotor flux. A plot of the product is shown below in Fig. 6.15.

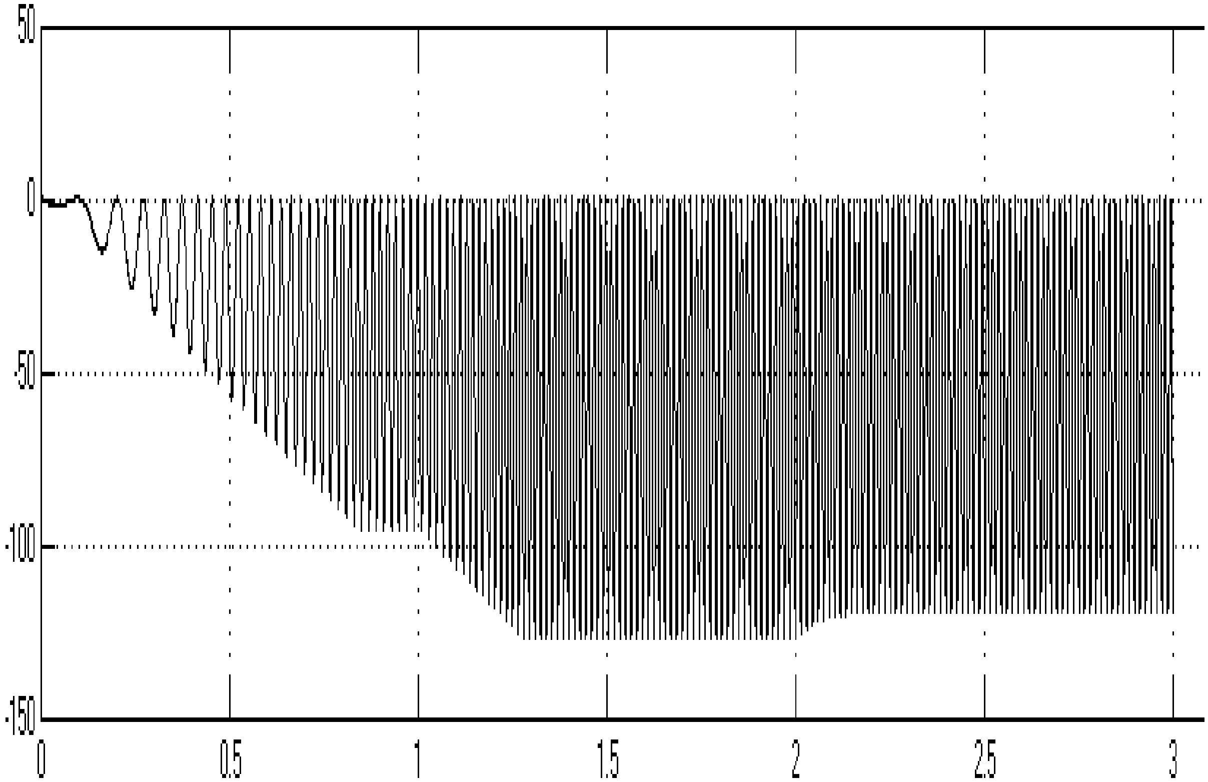

Fig. 6.15 Product of q component and derivative of d component of rotor flux.

The d component of the rotor flux is multiplied with the derivative of q component of the rotor flux. A plot of the product is given below in Fig. 6.16.

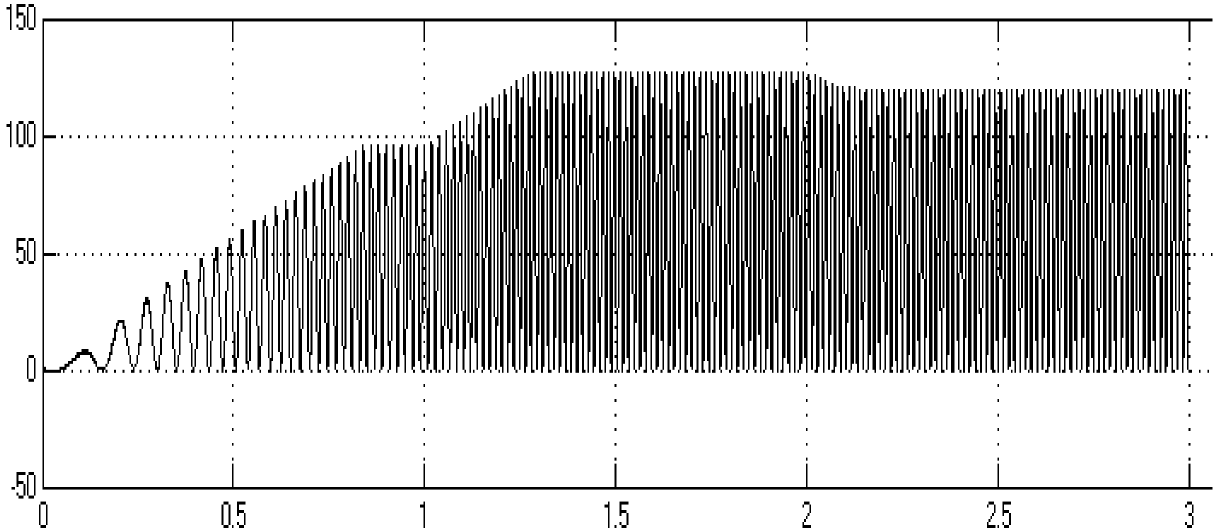

Fig. 6.16 Product of d component and derivative of q component of rotor flux.

Comparing both the products is shown in Fig. 6.17.

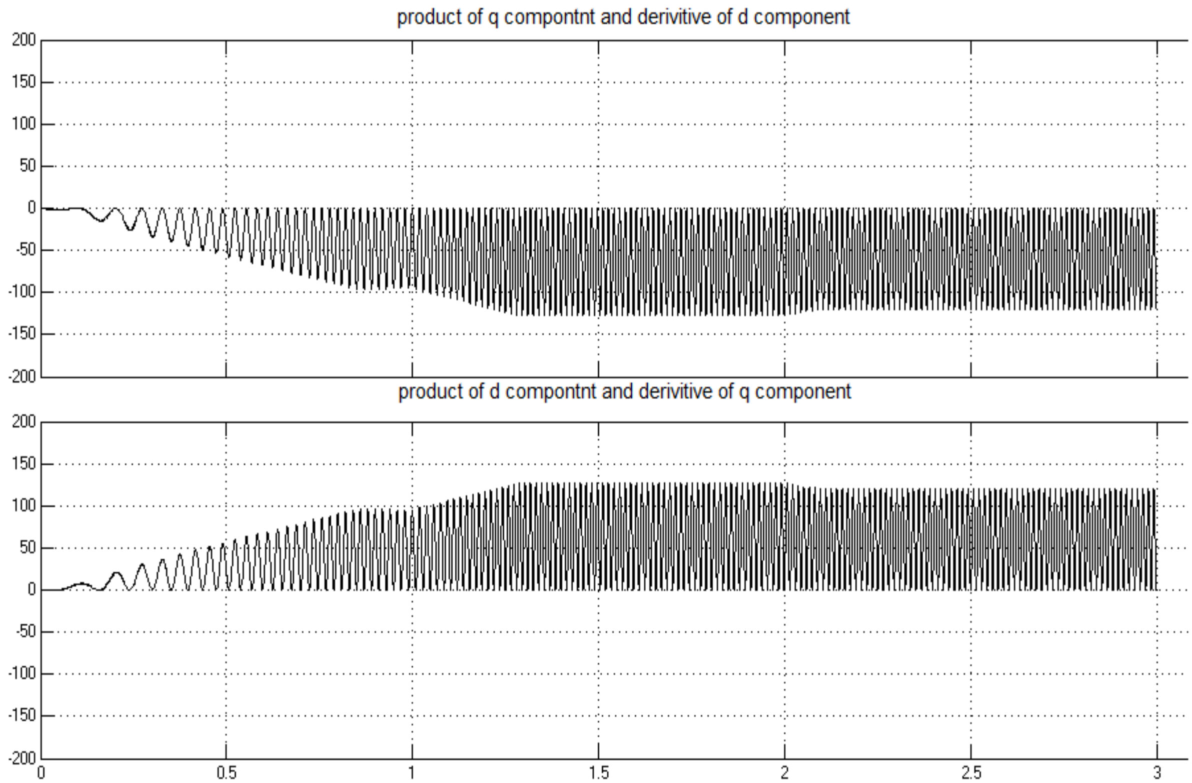

Fig. 6.17 Comparison of both the products of the fluxes.

From the above plot is can be observed that the waveforms are inverse to each other because of the d and q components are being multiplied with the derivatives of q and d components respectively.

The difference of the products is shown below in Fig. 6.18.

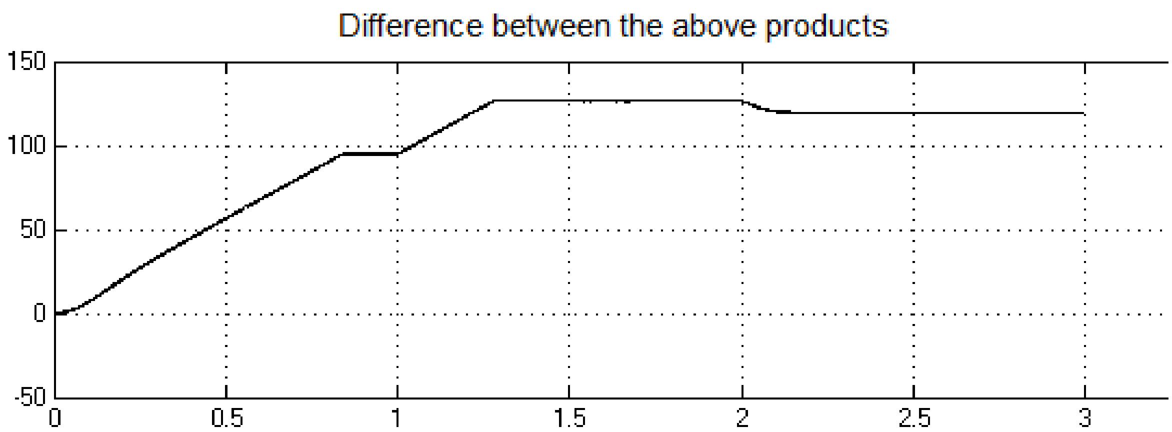

Fig. 6.18 Difference of the products of the fluxes.

The rotor flux squares are shown in Fig 6.19.

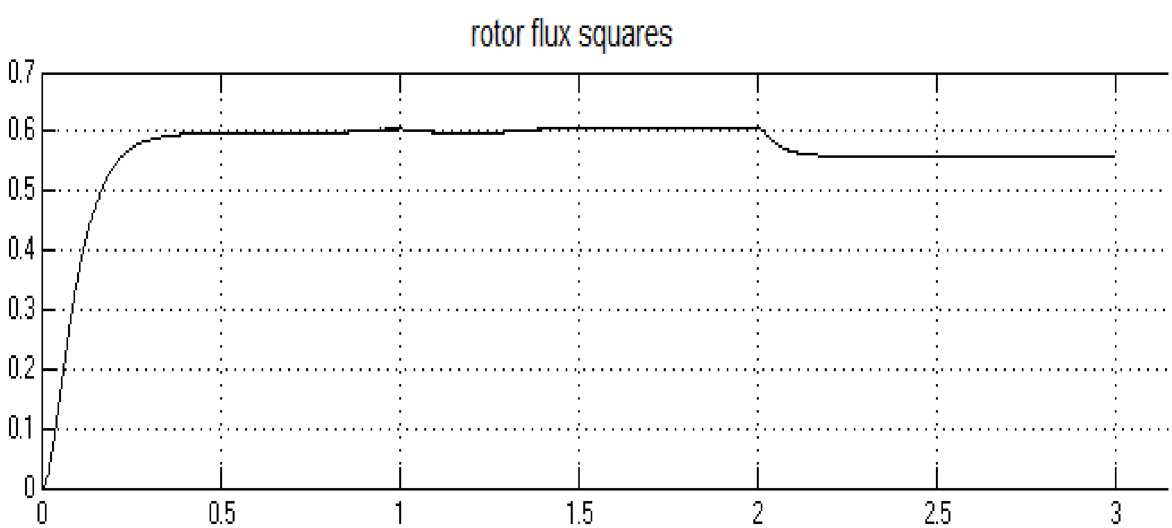

Fig. 6.19 Squares of the rotor flux.

The difference between the products of the dq components of the rotor flux as observed from Fig. 6.18 is divided by the square of the rotor flux as seen in Fig. 6.19. The resultant is the electrical frequency of the induction motor.

The electrical frequency of the induction motor is shown in Fig. 6.20.

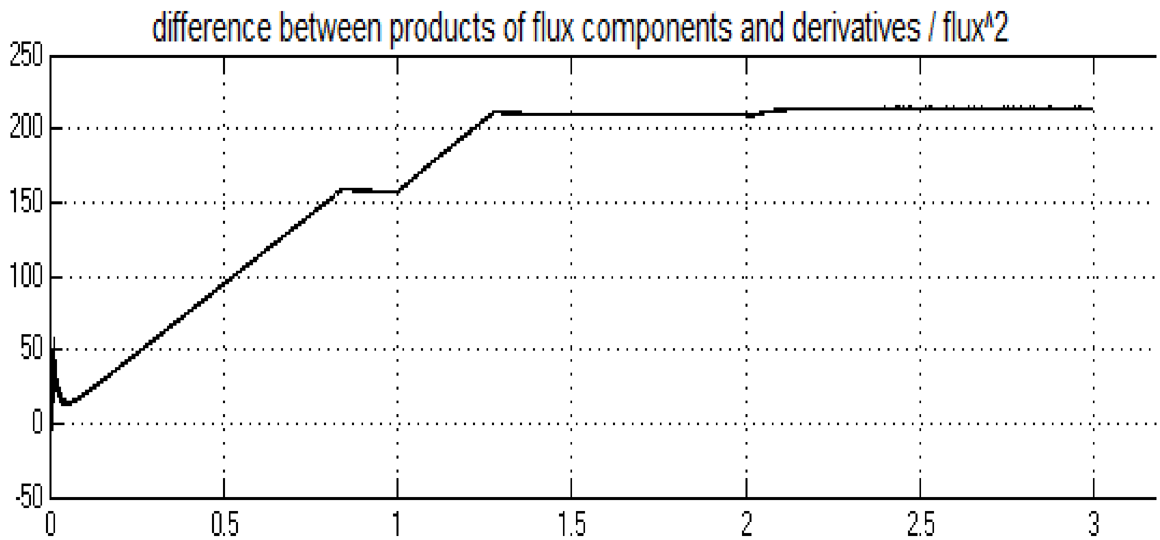

Fig. 6.20 Electrical frequency of the machine.

The electrical frequency of the machine is in rad/sec. It is divided with the number of pole pairs to get the synchronous speed of the machine.

The number of poles of the induction machine used is 4. So the count of the pole pairs is 2. Hence, the electrical frequency is divided by 2 to get the synchronous speed of the machine.

The below Fig.6.21 shows the plot of the synchronous speed of the motor.

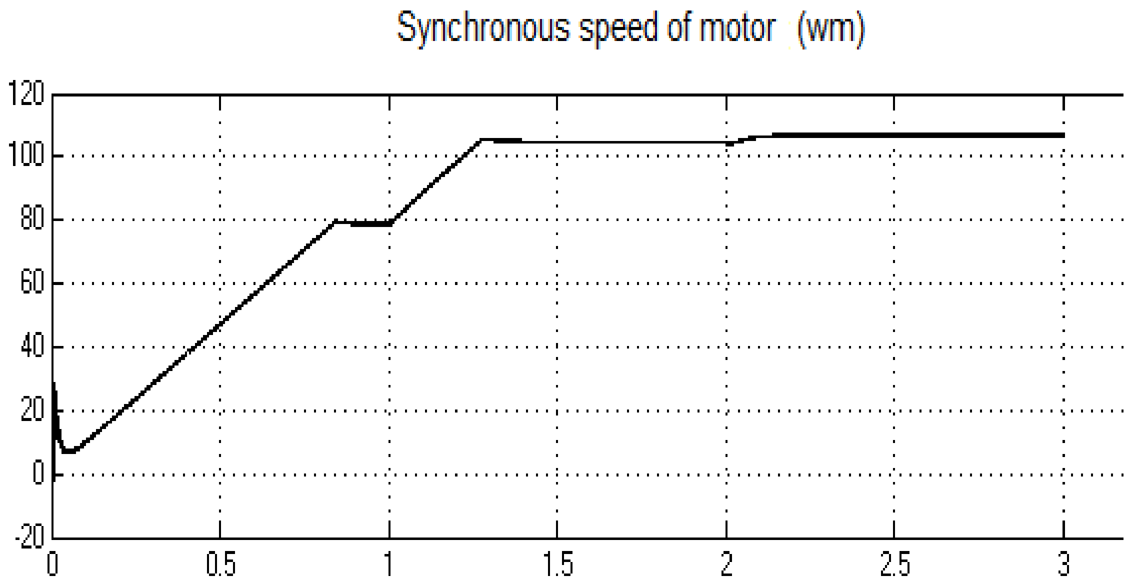

Fig. 6.21 Synchronous speed of the machine.

From equation 5.6, we know that slip frequency is the difference of electrical speed and the actual speed of the motor, i.e.,

$$S = Ns - Nr \tag{5.6}$$

The rotor speed (actual speed) of the motor is in rad/sec. Also, the synchronous speed of the motor is in rad/sec. Hence no conversion is needed to calculate the slip frequency.

The below Fig.6.22 shows the slip frequency of the motor.

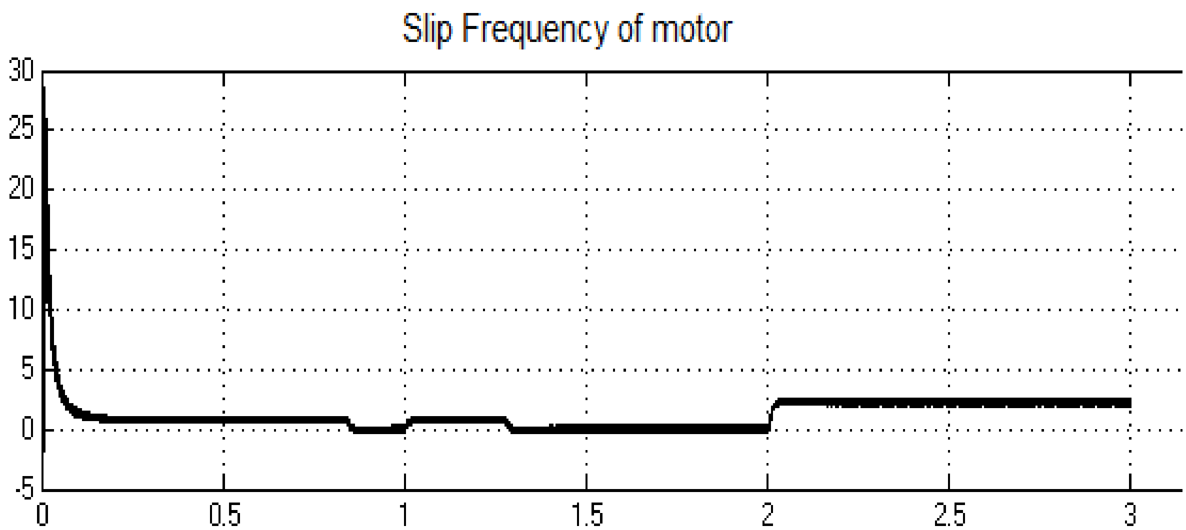

Fig. 6.22 Slip frequency of the induction motor using dq components of the flux and their derivatives.

Now, let's compare both the slip frequencies obtained from the slip frequency and from the flux derivatives. Figure 6.23 shows the comparison between the slip frequency of the induction motor obtained from two techniques.

From Fig.6.23 the first axis is the slip frequency from slip estimator and the second axis is calculated from the flux derivatives.

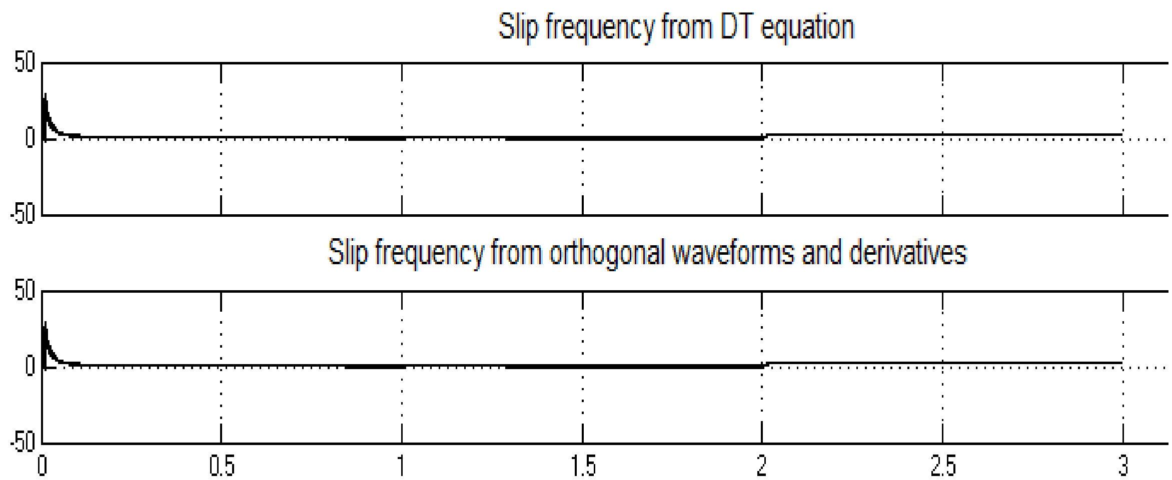

Fig. 6.23 Comparison of slip frequencies from both techniques.

As we can observe from the above Fig. 6.23, both the slip frequencies obtained from slip estimator based on torque equation and dq coordinates of rotor fluxes, respectively, are identical. The initial increase in the slip frequency when the motor is just started is noted to be approximately at 0.05 sec.

CHAPTER 7

CONCLUSIONS

As discussed in the previous chapters, the slip estimator using torque equation depends on the rotor resistance value. When the machine is operating, the machine gets heated up and the rotor resistance value may change, giving inaccurate slip value.

On the other hand, the second technique uses only the d and q components of the flux values and their derivatives. Hence, even though the second method is a little bit tricky, it is more reliable for the slip calculation.

Future Work:

As the slip frequency thus obtained has some harmonics, an analog to digital converter such as a Sigma-Delta converter can be employed, thus improving the resolution of the slip frequency.

REFERENCES

Chikhi , A., Mohamed , D., & Chikh, K. (2010). A comparative study of field-oriented control and direct-torque control of induction motors using an adaptive flux observer. *Serbian Journal of Electrical Engineering, 7*(1), 41-55.

Karlis, A., Kiriakopoulos, K., & Papadopoulos, D. (2006). Comparison of the Field Oriented and Direct Torque Control Methods for Induction Motors used in Electric Vehicles. *Laboratory of Electrical Machines, Department of Electrical and Computer Engineering, Democritus University of Thrace.*, 1-2.

Manney, D. (2013, March 29). *What Is Induction Motor Slip?* Retrieved from L&S ELECTRICINC: http://www.lselectric.com/what-is-induction-motor-slip/

MathWorks. (n.d.). (The Mathworks, Inc.) Retrieved March 03, 2016, from http://www.mathworks.com/help/physmod/sps/powersys/ref/directtorquecontroller.html?searchHighlight=speed%20controller%20for%20induction%20motor#responsive_offcanvas

Mathworks. (n.d.). *MathWorks*. (The MathWorks, Inc.) Retrieved March 03, 2016, from http://www.mathworks.com/help/physmod/sps/powersys/ug/simulating-an-ac-motor-drive.html#f4-7795

MathWorks. (n.d.). *MathWorks*. (The MathWorks, Inc.) Retrieved March 19, 2016, from http://www.mathworks.com/help/physmod/sps/powersys/ref/speedcontrollerac.html?s_tid=srchtitle#buu6f_d-2

Nemec, M., Nedeljkovic, D., & Ambrozic, V. (2007). Predictive torque control of induction machines using immediate flux control. *Industrial Electronics, IEEE Transactions on, 54(4)*, 2009-2017.

SARUTECH. (2016, March 3). *Electrical Study App*. (SARU TECH) Retrieved March 3, 2016, from http://electricalstudy.sarutech.com/field-oriented-control/index.html#Basic-Module-for-Field-Oriented-Control

Slip Speed in an Induction Motor. (n.d.). Retrieved from CIRCUIT GLOBE: http://circuitglobe.com/slip-speed-in-induction-motor.html